ABSTRACT

Title of Thesis:	**Control and Stabilization of Soft Inverted Pendulum on a Cart**
Name of Degree Candidate:	**Ananth Ajithkumar**
Degree and Year:	**Master of Science, 2023**
Thesis directed by:	**Dr. Nikhil Chopra** **Professor** **Department of Mechanical Engineering**

Underactuated systems are systems that cannot be controlled to track any arbitrary trajectories in their configuration space. In this work, we introduce a novel soft-robotic pendulum on a cart system. This is an underactuated soft-robotic system with two degrees of under-actuation. We model the system, derive the kinematics, and motivated by the control strategies for classical underactuated systems, we study the swing-up control and stabilization of this system around the vertical equilibrium point. The switching-based control law uses an energy-based control for swing-up and LQR for stabilization once the system is within the region of attraction of LQR. The simulation results depict the efficaciousness of the developed control scheme. Further, in this thesis, we discuss the viability and feasibility of feedback linearization, partially feedback-linearize the system and analyze the zero dynamics of the system.

Control and Stabilization of Soft Inverted Pendulum on a Cart

By

Ananth Ajithkumar

Thesis submitted to the Faculty of the Graduate School of the University of Maryland, College Park in partial fulfillment of the requirements for the degree of Master of Science

2023

Advisory Committee:

Professor Nikhil Chopra, Chair/Advisor

Professor Nuno C. Martins

Professor Behtash Babadi

Dedication

To my family, friends and loved ones.

Acknowledgements

I take this opportunity to express my deepest gratitude to my advisor Dr. Nikhil Chopra who took time out to hear and guide me in the right path and allow me to carry out the work through these years. Further, I am thankful to all the people who have helped me learn and make this thesis possible.

I would also like to thank my family and friends for their love and support

Table of Contents

List of Tables

List of Figures

List of Abbreviations and Acronyms

q_0	angle of curvature
θ	angle from vertical
x_p	position of the cart
L	length of the pendulum
D	width of the pendulum
m_c	mass of the cart
m_p	mass of the pendulum
g	acceleration due to gravity
K	kinetic energy
$D_{3\times3}$	inertia matrix
k	stiffness
$\beta_1,\ \beta_2$	damping constants
E	Energy

SIPC	soft inverted pendulum on a cart
SIPR	soft inverted pendulum with revolute base
LQR	linear quadratic regulator
PE	potential energy
KE	kinetic energy
SOS	sum of squares
LTI	linear time invariant

PBH Popov-Belevitch-Hautus

Chapter 1

1.1 Introduction.

The field of soft-robotics has been an area of interest for researchers for a long time. The recent explosion in the field of robotics has furthered research and development in the field. A robot is classified as hard or soft on the basis of the compliance of its underlying materials.

The physical characteristics of animals' bodies such as Elastic tendons, ligaments, and muscles enable animals to robustly interact with the external world and perform dynamic tasks[1]. The lack of rigid parts in the octopus body helps it to squeeze and manure through tight spaces. Similarly, the structure of an elephant's trunk helps it to grasp things easily. Similar features that are found in animals around us have made researchers incorporate those ideas into their design of robots. Further, the physical features of soft robots such as capability of continuum deformation allow researchers to mitigate many of the safety concerns associated with rigid body robots[2]. Hence, these bio-inspired robotic systems are used in rescue operations to medical surgeries.

The recent works in soft-robotics mainly focus on the control strategies for these under-actuated systems. These soft-robotic systems mostly being under-actuated makes the development of control laws difficult. One of the earlier works on

model based soft robotic control is discussed in [3] which for the first time tackles the development of closed loop dynamic controllers for a continuous soft robot.

This work mainly revolves around developing the control strategy of a novel soft robotic system on a cart inspired from the classical pendulum on a cart problem. This is a non-extensible soft-robotic arm with a revolving base on a cart. The motion of the cart is fixed to a single dimension. Hence the cart has a total of three dimensions of freedom, the curvature, the base angle and motion along the x-axis. In this work, only the curvature of the system is allowed to actuate. That is the angular acceleration of the base and acceleration of the cart cannot be controlled directly. This makes the system an underactuated system with two degrees of underactuation. Control strategies have been developed for soft robotic arms prior to this work. [5] and [6] deals with a similar soft robotic system in which the base of the system is fixed and the curvature is actuated. Hence the system has only one degree of freedom and is completely actuated. The system introduced in [4] has two degrees of freedom. Here, unlike in [5] and [6], the base is not fixed but the curvature is actuated. This gives the system an additional degree of freedom making it an underactuated system with one degree of under actuation. With an additional freedom of motion but with the same degree of actuation, the system dealt in this work becomes more complex and nonlinear.

In this work, we investigate the swing-up control for the soft robotic pendulum on a cart and its stabilization around the upright equilibrium point. Further, although feedback linearization is a well known strategy for the control of nonlinear

systems, it has not been employed in the control development of soft robotic underactuated systems. This work also investigates the viability of a feedback linearization for the problem described above and for a special case of the above problem where the mass of the cart goes to infinity. It should be noted that in the above-mentioned limiting case, the dynamics of the system considered in this work approaches the dynamics similar to [4] . In addition, it should also be noted that in the limit, i.e., when the mass of the cart goes to infinity and very high stiffness, the dynamics of the system converges to that of a classical pendulum.

Researchers have been dealing with control problems related to robotics for the past three decades. Due to the nature of dynamics, the control strategies that could be deployed for fully actuated systems cannot be directly implemented for underactuated systems[4] and hence novel methods need to be sought for the control of these systems.

Feedback linearization is one of the most widely used methods for the control of nonlinear systems. This method employs the use of a feedback to cancel out nonlinearities before the design of control laws. But, this cannot be used always since most of the systems do not satisfy the necessary conditions. For example, a simple classical pendulum is completely feedback linearizable while an acrobot or even the cart pole system is not completely feedback linearizable. To mitigate this problem, researchers came up with the idea of partial feedback linearization. Some of the earlier works in the field for the control of underactuated systems include control of acrobots using partial feedback linearization[7], pseudo

linearization using spline functions[8] and observer based pseudo linearization[9]. In [10] [11] and [12], the authors were successful in showing that partial feedback linearization can be used for swing up control of underactuated systems acrobot, and a class of gymnast robots.

The more recent method of control for underactuated systems is energy based control. This idea was first proposed in [13] for the swing up control of an underactuated cart pole system. [14]and [15] employ the use of similar energy based swing up control of the stabilization of more complex under actuated systems. In this work we will use a similar energy based approach for the swing up control of the system. Further, once the system reaches close to the upright position with the help of swing up control, we switch to a LQR controller to stabilize it around this equilibrium point.

1.2 Thesis Objective.

The objective of this work is to

- Derive the kinematics that corresponds to the novel soft robotic system with revolute base attached to a cart (SIPC system).
- Design an energy based swing-up control which would take the system from any arbitrary starting point in the configuration space to close to the upright equilibrium point.
- Stabilize the system around this equilibrium point.
- Analyze the robustness and sensitivity of this control strategy.

- Investigate the viability of feedback linearization and employ it for the control of a special case of the system.

1.3 Organization of Thesis

The thesis is organized as below.

In chapter two, we derive the dynamics of the soft robotic system with revolute base attached to a cart. We analyze the system with different values of system parameters. We also compare the dynamics of the system in the limiting case.

In chapter three, we deal with analysis of the system around the equilibrium point, derive the control law to stabilize the system around the equilibrium point, evaluate the sensitivity of the controller, and find the domain of attraction of the designed controller.

In chapter four, we develop the swing up control for the system, the necessary conditions for the swing up control to work, stability analysis of the obtained control law, and the robustness of the controller.

In chapter five we aim to control the system by canceling the nonlinearities of the system when the mass of the cart is very high. This can be regarded as a special case of the system. We investigate the viability of such a control law and try to implement it in the above context.

Chapter-2 Kinematics and Dynamics

2.1 Introduction

In this chapter, we derive the kinematics and dynamics of the soft robotic pendulum on a cart system. For this, first, we model the system, then find the kinetic and potential energy of the system, then formulate the Lagrangian and finally use the Lagrangian to formulate the equations of motion. Further, will investigate the properties and sensitivity of the above mentioned system.

2.2 System Model

To model the system we use the similar method used in [4]. We first model the soft-robotic pendulum and then interconnect it with the cart to model the entire system. To model the pendulum, consider the system in figure[1]. Before starting the modeling we make the following standard assumptions.

- The soft robotic pendulum is non-extensible with constant curvature..
- Both the cart and the pendulum have uniform densities.
- There is no loss of energy on the joint between the cart and the pendulum
- The pendulum cart system always remains attached to the ground and the cart makes an angle of zero degrees to the ground

To model the pendulum, let L be the length of the pendulum along its central axis, D be its thickness. Also, let us define s ϵ [0,1] such that L*s is the arc length along the robot's central axis to the point s from the base, and d ϵ [-0.5, 0.5] such that D*d is the lateral distance to the point d from the central axis. Let $\hat{S}_s$ be the reference frame at each point s along the soft body's axis. Hence, from the above parametrization, $\hat{S}_0$ will be the base frame and $\hat{S}_1$ will be the top most frame. Using this convention we can describe any point on the robot's body. For example, (s,d) = (0.5, 0.25) describes the point on frame $\hat{S}_{0.5}$ (frame that is half way on the robots central axis) at a distance of 0.25*D on the lateral side from the central axis.

Using the above mentioned constant curvature assumption (CC), we define the configuration variables of the pendulum system as $q_0(t) \in \mathbb{R}^1$ and $\theta(t) \in S^1$, such that $q_0(t) = L/r(t)$ where r(t) is the radius of curvature of the pendulum and $\theta(t)$ is the angle that base of the pendulum makes with the cart.

Therefore, the orientation of the frame $\hat{S}_s$ is given by,

$$\alpha_s(t) = \theta(t) + \int_0^s q_0(t)dl$$

$$= \theta(t) + q_0(t)l\Big|_0^s$$

$$= \theta(t) + q_0(t) * s \qquad (1)$$

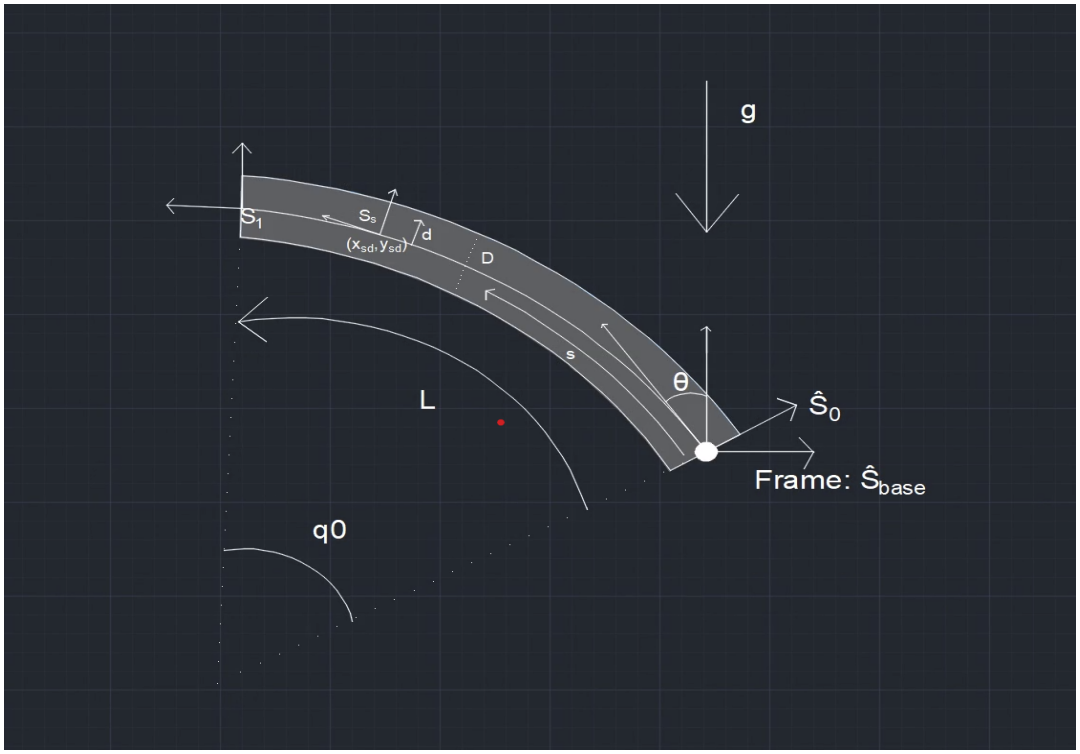

Figure: 2.1 Soft-robotic pendulum design.

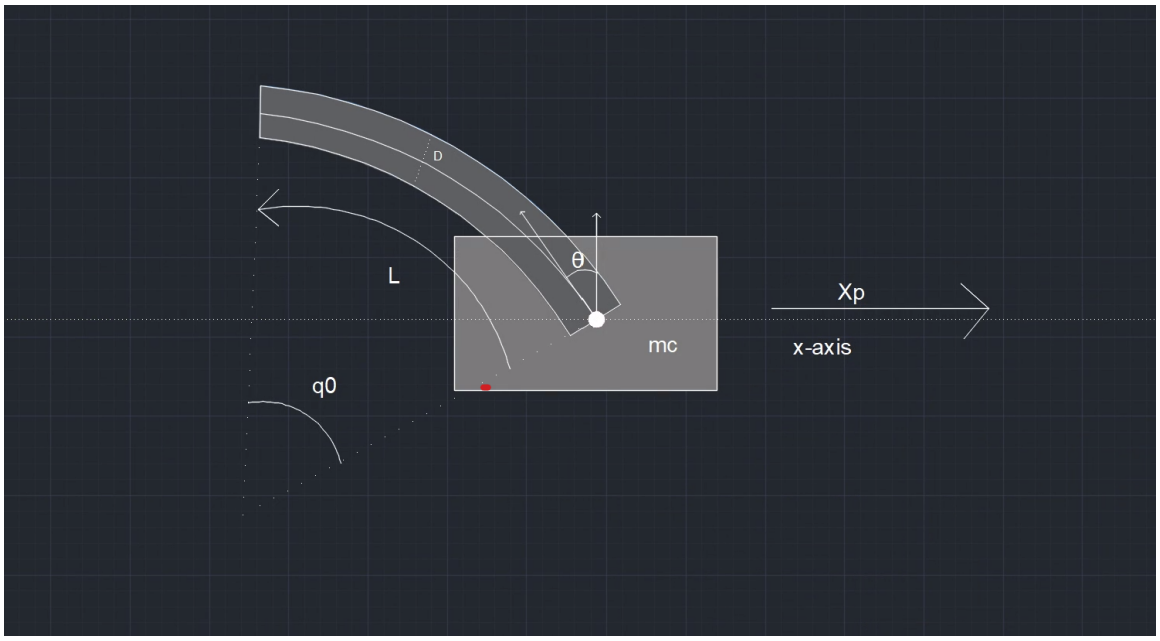

Figure: 2.2 Soft-robotic pendulum on a cart system.

Now, we find the cartesian coordinates x_{sd} and y_{sd} at a general point on the pendulum parametrized by s and d. From the above figure,

$$x_{sd} = Ddcos(\alpha_s(t)) + x^*_{sd} \tag{2}$$

$$y_{sd} = Ddsin(\alpha_s(t)) + y^*_{sd} \tag{3}$$

where,

$$\frac{dx^*_{sd}}{L} = cos(\frac{\Pi}{2} + \alpha_s(t))ds \tag{4}$$

$$\frac{dy^*_{sd}}{L} = sin(\frac{\Pi}{2} + \alpha_s(t))ds \tag{5}$$

Integrating both sides of (4) and (5), we get,

$$\frac{x^*_{sd}}{L} = \int_0^s - sin(\alpha_s(t))ds \, , \frac{y^*_{sd}}{L} = \int_0^s cos(\alpha_s(t))ds \tag{6}$$

$$x^*_{sd} = - L\int_0^s sin(\alpha_s(t))ds \tag{7}$$

$$y^*_{sd} = L\int_0^s cos(\alpha_s(t))ds \tag{8}$$

Substituting equations (7) and (8) back into (4) and (5) gives,

$$x_{sd} = Ddcos(\alpha_s(t)) - L\int_0^s sin(\alpha_s(t))ds \tag{9}$$

$$y_{sd} = Ddsin(\alpha_s(t)) + L\int_0^s cos(\alpha_s(t))ds \tag{10}$$

Now, consider the case where this pendulum is attached to the cart. This allows the pendulum to have another degree of freedom along the x-axis. This gives the

system another configuration variable x_p where $x_p \epsilon \mathbb{R}^1$ denotes the location of origin of the pendulum.

Finally, the position of any arbitrary point on the pendulum at any orientation of the system is given by,

$$x_{sdx} = Ddcos(\alpha_s(t)) - L\int_0^s sin(\alpha_s(t))ds + x_p \tag{11}$$

$$y_{sdx} = Ddsin(\alpha_s(t)) + L\int_0^s cos(\alpha_s(t))ds + h \tag{12}$$

where h denotes the height of the base of the pendulum from the x-axis.

Now, since we have the general cartesian coordinate of the system, we can go on to derive the dynamics of the system.

2.3 Dynamics

In this section, we derive the expression for kinetic energy, potential energy, formulate the lagrangian and finally derive the equations of motion. In this work, we will calculate the kinetic energy contribution by the pendulum and cart independently and add them to find the total kinetic energy of the system.

On integrating and simplifying (11) and (12) we get,

$$x_{sdx} = Ddcos(\theta(t) + q_0(t)s) + \frac{L}{q_0(t)}(cos(\theta(t) + q_0(t)s) - cos(\theta(t)) + x_p \tag{13}$$

$$y_{sdx} = Ddsin(\theta(t) + q_0(t)s) + \frac{L}{q_0(t)}(sin(\theta(t) + q_0(t)s) - sin(\theta(t)) + h$$

(14)

Now, the kinetic energy of the point characterized by (s,d) on the pendulum is given by,

$$\bigtriangledown K_p = \frac{1}{2}\rho(s,d) * (\dot{x}_{sdx}^2 + \dot{y}_{sdx}^2) \quad (15)$$

where $\dot{x}_{sdx}$ and $\dot{y}_{sdx}$ are the time derivatives of x_{sdx} and y_{sdx} and such that,

$$\int_0^1 \int_{-0.5}^{0.5} \rho(s,d) dd\, ds = m_p$$

Since we are dealing with uniform density, $\rho(s,d)=\rho$. Further, from (15),

$$K_p = \frac{1}{2}\int_0^1 \int_{-0.5}^{0.5} \rho * (\dot{x}_{sdx}^2 + \dot{y}_{sdx}^2) dd\, ds \quad (16)$$

where K_p is the kinetic energy of the pendulum.

Now, the kinetic energy of the cart can be directly written as,

$$K_c = \frac{1}{2} m_c \dot{x}_p^2 \quad (17)$$

On summing 16 and (17), we get the total energy of he cart,

$$KE = \frac{1}{2}\int_0^1 \int_{-0.5}^{0.5} \rho * (\dot{x}_{sdx}^2 + \dot{y}_{sdx}^2) dd\, ds + \frac{1}{2} m_c \dot{x}_p^2 \quad (18)$$

On simplifying (18) we get the kinetic energy of the system. For concise representation this total kinetic energy can represented as

$KE = \frac{1}{2}\dot{q}^T D(q)\,\dot{q}$ where $\dot{q}$ is the time derivative of $\dot{q} = [\dot{q}_0(t),\ \dot{\theta}(t),\ \dot{x}_p(t)]^T$.

The matrix D(q) $\epsilon\ \mathbb{R}^{3x3}$ is called the inertia matrix. In the upcoming sections, we will discuss the properties of this matrix.

$$D = \begin{bmatrix} D_{11} & D_{12} & D_{13} \\ D_{21} & D_{22} & D_{23} \\ D_{31} & D_{32} & D_{33} \end{bmatrix} \tag{19}$$

Please refer appendix for the terms of the matrix

Now, we derive the potential energy of the system. The potential energy of the system is the sum of potential energy of the cart and the soft robotic pendulum. Since the cart is always assumed to slide on the x-axis, the potential energy of the cart is zero. Therefore, the total potential energy of the combined system is just the potential energy of the pendulum. I.e.,

$$PE = m_p g \int_0^1 \int_{-0.5}^{0.5} (x_{sdx} sin(\eta) + y_{sdx} cos(\eta)) dd\, ds \tag{20}$$

where g is the acceleration due to gravity. In this work, we have set η, the direction of the gravitational field as zero. Now, substituting y_{sdx} from equation (14) and simplifying we get,

$$PE = -\frac{Lgm_p cos(q_0 + \theta) - Lgm_p cos(\theta) + Lq_0 gm_p sin(\theta)}{q_0^2} \tag{21}$$

Now we can define the Lagrangian.

Lagrangian is defined as the difference between kinetic and potential energy.

i.e., $L = KE - PE$

$$= \frac{1}{2}\dot{q}^{T} D(q)\ \dot{q} + \frac{Lgm_p cos(q_0 + \theta) - Lgm_p cos(\theta) + Lq_0 gm_p sin(\theta)}{q_0^2} \qquad (22)$$

Now, the Euler-Lagrange equation

$$\frac{\partial L}{\partial q^{i}}(t, q(t), \dot{q}(t)) - \frac{d}{dt}\frac{\partial L}{\partial \dot{q}^{i}}(t, q(t), \dot{q}(t)) = \tau_i, \quad i = 1, 2, 3 \ldots\ldots\ldots n \qquad (23)$$

can be used to derive the equations of motion of the system where

$$q^1 = q_0(t),\ q^2 = \theta(t)\ and\ q^3 = x_p(t)$$

From [16] we can rewrite the Euler-Lagrange equation (23) as

$$\sum_{j=1}^{n} d_{kj}(q)\ddot{q}_j(t) + \sum_{i=1}^{n}\sum_{j=1}^{n} c_{ijk}(q)\dot{q}_i\dot{q}_j + g_k(q) = \tau_k \qquad k = 1, 2 \ldots\ldots\ldots n, \qquad (24)$$

where $g_k = \frac{\partial PE}{\partial q_k}$ and $c_{ijk} = \frac{1}{2}\left\{\frac{\partial d_{kj}}{\partial q_i} + \frac{\partial d_{ki}}{\partial q_j} - \frac{\partial d_{ij}}{\partial q_k}\right\}$, $d_{kj} \epsilon\, D(q)$. The terms c_{ijk} known as Christoffel symbols. The terms of type $\dot{q}_i\dot{q}_j$ are called Coriolis terms while the terms of type $\dot{q}_i^{2}$ are called the centrifugal terms. The above analysis applies to all system whose kinetic energy is of the form $KE = \frac{1}{2}\dot{q}^{T} D(q)\ \dot{q}$

Finally the above equation (24) can be written as

$$D(q)\ \ddot{q}(t) + C(q, \dot{q})\dot{q} + G(q) = \tau \qquad (25)$$

Now, for the system discussed in this work, $n = 2$, $q = \left[q_0(t),\ \theta(t),\ x_p(t)\right]^T$, $\dot{q} = \left[\dot{q}_0(t),\ \dot{\theta}(t),\ \dot{x}_p(t)\right]^T$ and $\ddot{q}_0(t) = \left[\ddot{q}_0(t),\ \ddot{\theta}(t),\ \ddot{x}_p(t)\right]^T$. Substituting for D in equation (24), solving and writing it in (25) form, we get,

$$C(q,\ \dot{q}) = \begin{bmatrix} C_{11} & C_{12} & C_{13} \\ C_{21} & C_{22} & C_{23} \\ C_{31} & C_{32} & C_{33} \end{bmatrix}$$

Please refer to the appendix for the elements of the matrix.

Further,

$$G(q) = \begin{bmatrix} G_1 \\ G_2 \\ G_3 \end{bmatrix} \text{ where,}$$

$$G_1(q) = \frac{Lgm_p(2cos(q_0+\theta)-2cos(\theta)+q_0 sin(q_0+\theta)+q_0 sin(\theta))}{q_0^3}$$

$$G_2(q) = -\frac{Lgm_p(sin(\theta)-q_0 cos(\theta)+q_0 cos(\theta))}{q_0^2}$$

$$G_3(q) = 0$$

Finally, on adding the damping and stiffness terms we get,

$$D(q)\ \ddot{q}(t) + C(q,\dot{q})\dot{q} + B_\beta \dot{q} + K_k q + G(q) = \tau \qquad (26)$$

Where the damping $B_\beta = \begin{bmatrix} \beta_1 & 0 & 0 \\ 0 & 0 & 0 \\ 0 & 0 & \beta_2 \end{bmatrix}$,

the stiffness term $K = \begin{bmatrix} k & 0 & 0 \\ 0 & 0 & 0 \\ 0 & 0 & 0 \end{bmatrix}$, and $\tau = \begin{bmatrix} \tau_1 \\ \tau_2 \\ \tau_3 \end{bmatrix}$

Properties of D(q) and $C(q,\dot{q})$

- It should be noted that D(q) is a positive definite symmetric matrix, i.e., $x^T Dx > 0,\ \forall\, x \in \mathbb{R}^n$
- Further, the matrix $N(q,\dot{q}) = \dot{D(q)} - 2C(q,\dot{q})$ is skew-symmetric. That is $n_{jk} = -\, n_{kj}$
- D(q) is bounded. i.e., $\exists a > 0\ and\ b > 0\ st\ a < D(q) < b$

Finally from (25) we get the equations of motion.,

$$\ddot{q(t)} = D(q)^{-1}(\tau - (C(q,\dot{q})\dot{q} + B_\beta \dot{q} + K_k q + G(q))) \qquad (27)$$

Dynamics when $q_0(t) = 0$.

It should be noted that the inertia matrix(D), the coriolis matrix($C(q,\dot{q})$), and the potential energy differential(G(q)) has terms with division by $q_0(t)$. This might cause the D-matrix and C-matrix to explode when $q_0(t)$ goes to zero. But, for the system the limit of D, C and G matrices exist and are finite. The limit values of these two matrices are given below.

$$\lim_{q_0 \to 0} D(q_0) = \begin{bmatrix} D_{11} & D_{12} & D_{13} \\ D_{21} & D_{22} & D_{23} \\ D_{31} & D_{32} & D_{33} \end{bmatrix} \text{ where,} \qquad (28)$$

$$D_{11} = \frac{m_p(9L^2 + 5D^2)}{180}, \quad D_{12} = \frac{m_p(3L^2 + D^2)}{24}, \quad D_{13} = \frac{Lm_p cos(\theta)}{6},$$

$$D_{21} = \frac{m_p(3L^2 + D^2)}{24}, \quad D_{22} = \frac{m_p(4L^2 + D^2)}{12}, \quad D_{23} = -\frac{Lm_p cos(\theta)}{2},$$

$$D_{31} = \frac{Lm_p cos(\theta)}{6}, \quad D_{32} = -\frac{Lm_p cos(\theta)}{2}, \quad D_{33} = m_c + m_p,$$

$$\lim_{q_0 \to 0} C(q_0, \dot{q_0}) = \begin{bmatrix} 0 & 0 & 0 \\ 0 & 0 & 0 \\ \frac{Lm_p sin(\theta)(\dot{q_0} + 2\dot{\theta})}{12} & \frac{Lm_p sin(\theta)(\dot{q_0} + 3\dot{\theta})}{6} & 0 \end{bmatrix} \quad (29)$$

$$\lim_{q_0 \to 0} G(q) = \begin{bmatrix} \frac{-Lm_p g \sin(\theta)}{6} \\ \frac{-Lm_p g \sin(\theta)}{2} \\ 0 \end{bmatrix} \quad (30)$$

Now, consider the case when $q_0 \equiv 0$ which means $\dot{q_0} = 0$ and $\ddot{q_0} = 0$. Therefore, from (26) we get three equations. The second and third equations are shown below. We have skipped the first equation since it is the same as the second equation.

$$\frac{\ddot{\theta} m_p (3L^2 + D^2)}{12} - \frac{L \ddot{x_p} m_p cos(\theta)}{2} - \frac{L g m_p sin(\theta)}{2} = 0,$$

$$\frac{L m_p sin(\theta) \dot{\theta}^2}{2} + \ddot{x_p}(m_c + m_p) - \frac{L \ddot{\theta} m_p cos(\theta)}{2} = 0$$

The above two equations are analogous to the equation of motion of the cart pole system. This is highly intuitive because when the curvature of the pendulum is set to zero, the pendulum behaves like a pole of length L and width D.

Now we define the system parameters that we used for simulation. The length, width and mass of the pendulum, the mass of the cart and beta and K values are given below in Table-1.

Parameters	**Values**
L (length)	1.00m

g (acceleration due to gravity	9.8 m/s^2
k (stiffness)	0.5 N/m
β_1 (damping constant)	0.11 Ns/m
β_2 (damping constant)	0.1 Ns/m
D (width of robotic pendulum)	0.1 m
m_c (mass of the cart)	1 kg
m_p (mass of the pendulum)	2 kg

Table:1 System Parameters

2.4 Simulation Results

The dynamics of the system in the absence of any external input is shown in the figures below. The system was initialized from the starting point [pi/2;pi/2;0 ;0;0;0].

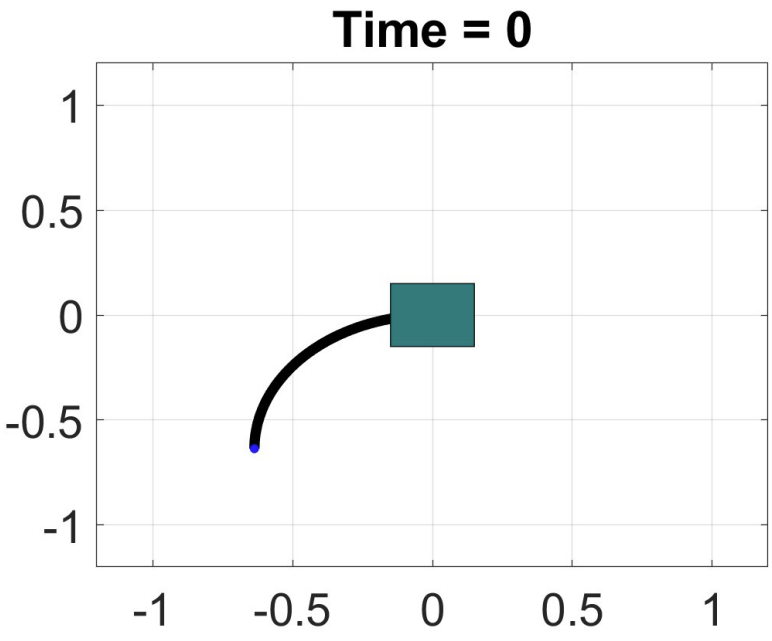

Figure: 2.3 Moments after the pendulum started from the initial state

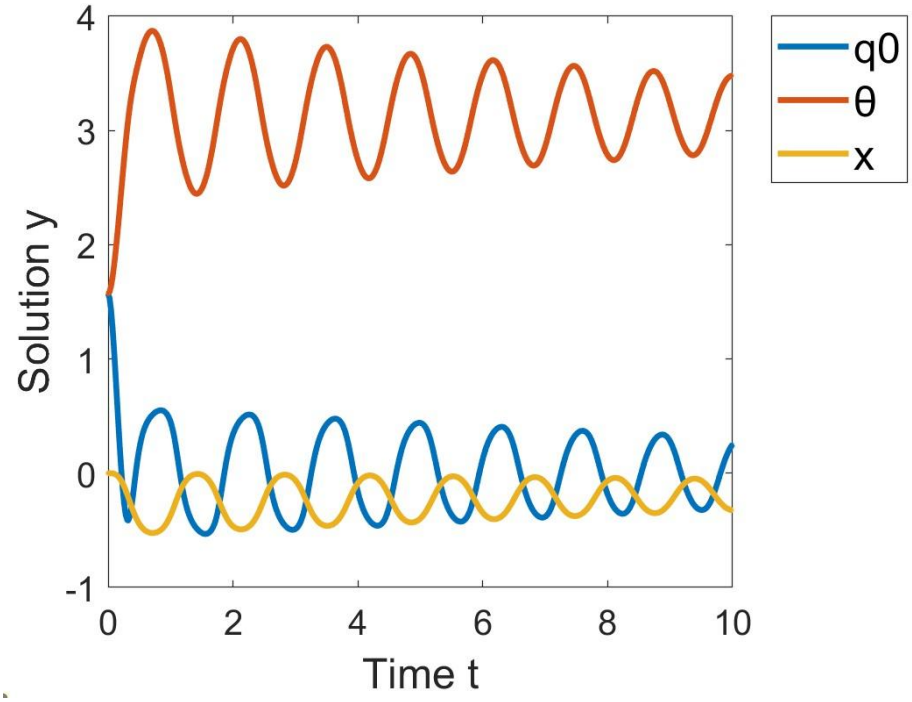

Figure: 2.4 Dynamics of the system with damping

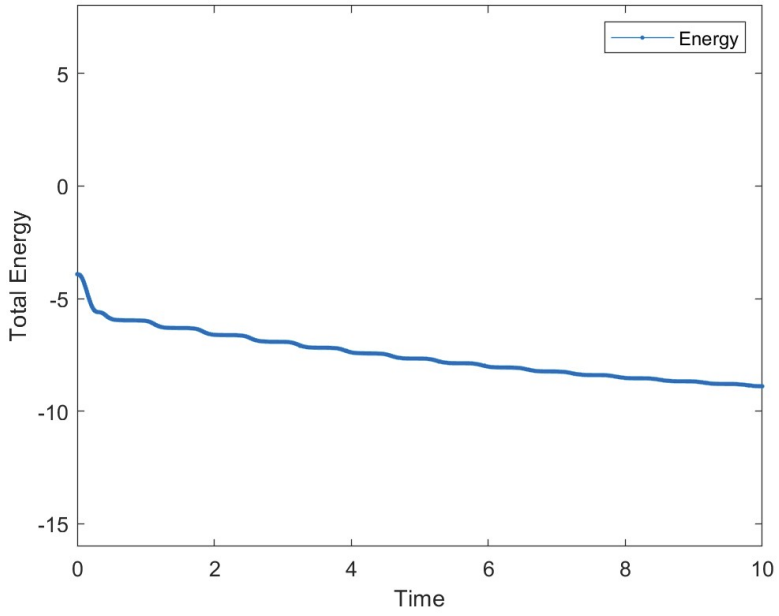

Figure: 2.5 Total energy of the system with damping.

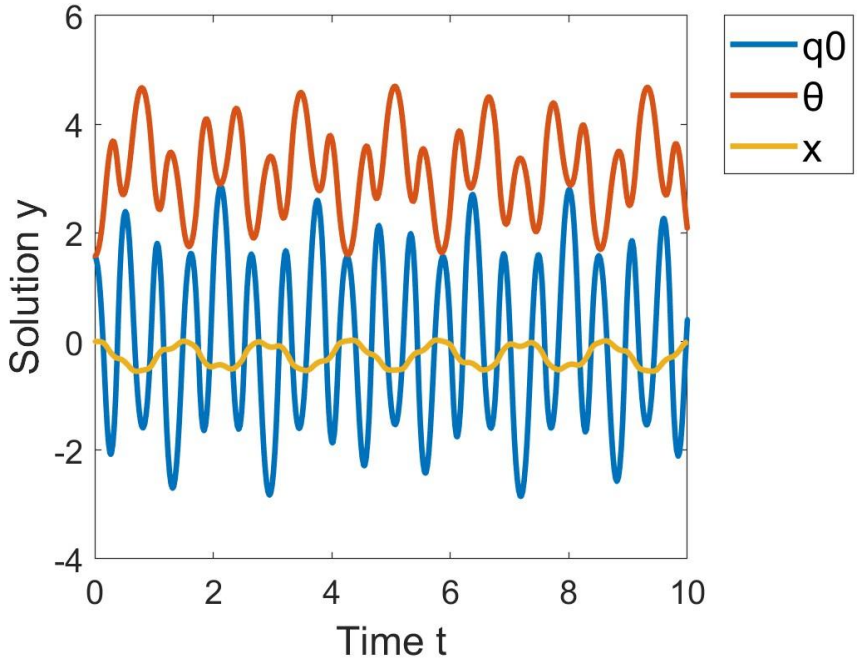

Figure: 2.6 Dynamics of the system without damping

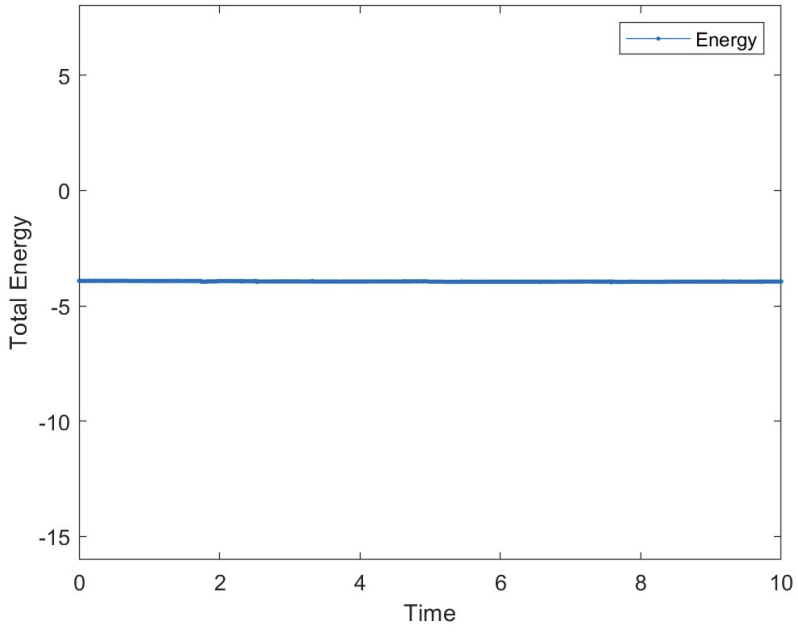

Figure: 2.7 Total energy of system without damping

It should be noted that the energy of the system in downward position is $-\frac{m_p gL}{2}$. (This is further discussed in chapter-4). Figure-5 and 6 shows the dynamics and energy of the system. As we can see from figure-5, the system which was initialized from [pi/2;pi/2;0 ;0;0;0] is slowly approaching equilibrium because of damping. As expected, the total energy of the system is reducing and slowly approaching -9.8J which corresponds to the energy of the system when it is in the stable equilibrium.

The same simulation was conducted for the un-damped system. This can easily be achieved by setting the B_β matrix and K_k matrix to zero. The dynamics and total energy of this system are given in figure-6 and figure-7. As expected, the total energy of the system was constant in this case. Figure-6 shows the undamped oscillations and figure-7 shows that the energy of the system is constant.

2.5 Summary

This chapter focused on the derivation of kinematics and dynamics of the system. We used the method similar to the one used in [3] and [4] to derive the dynamics and the Lagrange method to derive the dynamics. Now, the dynamics given by (27) can be used to develop the control laws for the system.

Chapter-3 Stability Analysis and Stabilization

3.1 Introduction

In this chapter we will start with writing the system dynamics (27) in state- space form, find the equilibrium points, analysis of the system around its equilibrium points, linearize the system around the equilibrium point, derive a control law to stabilize the system around the equilibrium point, evaluate the sensitivity of the controller, and find the domain of attraction of the designed controller.

3.2 State Space form

First, we will write the system is equation (27) in standard form,

$$\dot{x} = f(x) + g(x)u \tag{31}$$

Where u is the control input.

We know $\frac{dq_0}{dt} = \dot{q}_0, \frac{d\dot{q}_0}{dt} = \ddot{q}_0, \frac{d\theta}{dt} = \dot{\theta}, \frac{d\dot{\theta}}{dt} = \ddot{\theta}, \frac{dx_p}{dt} = \dot{x}_p, \frac{d\dot{x}_p}{dt} = \ddot{x}_p$ (32)

i.e., from 32 and 27 we get

$$\dot{x} = \begin{bmatrix} \dot{q_0} \\ \dot{\theta} \\ \dot{x_p} \\ [D(q)^{-1}(\tau - (C(q,\dot{q})\dot{q} + B_\beta \dot{q} + K_k q + G(q)))]_{3X1} \end{bmatrix}_{6X1} \tag{33}$$

$$= \begin{bmatrix} \dot{q_0} \\ \dot{\theta} \\ \dot{x_p} \\ [D(q)^{-1}(-(C(q,\dot{q})\dot{q} + B_\beta \dot{q} + K_k q + G(q)))]_{3X3} \end{bmatrix}_{6X1} + \begin{bmatrix} 0 \\ 0 \\ 0 \\ [D(q)^{-1}\tau]_{3X1} \end{bmatrix}$$

Where $\tau = \begin{bmatrix} \tau_1 \\ \tau_2 \\ \tau_3 \end{bmatrix}$.

It should be noted that when $m_p \to \infty \Rightarrow \ddot{x}_p \to 0$. This means that $\dot{x}_p = c$, where c is some constant ($c \in \mathbb{R}^1$). If we are starting from rest then $\dot{x}_p = c = 0$ which means that $x_p = l$ where l is some constant $\in \mathbb{R}^1$. Assume that $x_p(0) = 0$, i.e., we are starting from the origin. Substituting these values of x_p and $\dot{x}_p$ back in equation (33) we get the system described in [4]. It is not surprising because even for the pendulum on a cart system, if the mass of the cart is made "infinity" then the dynamics of the system converges to that of just the pendulum.

Now we have our system in standard form. The state-space of the system is six dimensional. That is, there are 6 state variables namely the angle of curvature (q_0), the angle from the origin (θ), the displacement along x-axis (x_p), the angular velocity of the curvature ($\dot{q}_0$), the angular velocity of the angle from vertical ($\dot{\theta}$) and finally the velocity along the x-axis ($\dot{x}_p$).

The next task is to find the equilibrium point. The necessary condition for the equilibrium point is that the unforced system has $\dot{x} = 0$. i.e., $f(x) = 0$. Substituting this condition in equation (33) and solve for the state variables

$$x = \left[q_0(t),\ \theta(t),\ x_p(t),\ \dot{q}_0(t),\ \dot{\theta}(t),\ \dot{x}_p(t)\right]^T \tag{34}$$

we get the equilibrium points.

The equilibrium points of the system are

$$\left[0, 0, x_p, 0, 0, 0\right] \text{ and } \left[0, n\pi, x_p, 0, 0, 0\right],\ x_p \in \mathbb{R}^1,\ n \in Z \tag{35}$$

This makes sense because for the isolated system (no influence of external force) as long as

$$\dot{q}_0,\ q_0,\ \dot{\theta}, \text{ and } \dot{x}_p \text{ are zero and } \theta = n\pi \tag{36}$$

the position of the cart does not affect the equilibrium point. As long as the above conditions are satisfied, irrespective of where the soft-robotic pendulum system is, it is in equilibrium. It should be noted that the equilibrium point $\left[0, n\pi, x_p, 0, 0, 0\right]$ is stable for $\theta = (2n + 1)\pi,\ n \in Z$ (vertically down state) and is unstable for $\theta = 2n\pi,\ n \in Z$ (upright state). More about the stability will be discussed in the next section. However in this work we are interested in stabilizing the pendulum around the origin. Therefore we are interested in the equilibrium point

$$x_0 = \left[q_0(t),\ \theta(t),\ x_p(t),\ \dot{q}_0(t),\ \dot{\theta}(t),\ \dot{x}_p(t)\right] = [0, 0, 0, 0, 0, 0] \tag{37}$$

i.e., when the soft pendulum is in the inverted state.

In this work we will try to control the system with two degrees of underactuation. Therefore, we will be trying to stabilize the system by varying just the curvature. Therefore,

$$\tau = \begin{bmatrix} \tau_1 \\ \tau_2 \\ \tau_3 \end{bmatrix} = \begin{bmatrix} \tau_1 \\ 0 \\ 0 \end{bmatrix} \tag{38}$$

3.3 Stability Analysis

To find the stability of the equilibrium point of our interest, we follow the methods discussed in [17] and [18]

First we need to linearize the system.

Theorem-1: From [17], for the nonlinear system

$$\dot{x} = f(x,u),\ y = g(x,u),\ x \in \mathbb{R}^n,\ u \in \mathbb{R}^k,\ y \in \mathbb{R}^m$$

Where x are the state variables and u are the control inputs, the LTI system,

$$\dot{\delta x} = A\delta x + B\delta u,\ \delta y = C\delta x + D\delta u \tag{38}$$

defined by the following Jacobian matrices

$$A := \frac{\partial f(x^{eq},u^{eq})}{\partial x},\quad B := \frac{\partial f(x^{eq},u^{eq})}{\partial u},\quad C := \frac{\partial g(x^{eq},u^{eq})}{\partial x},\quad D := \frac{\partial g(x^{eq},u^{eq})}{\partial u} \tag{39}$$

Is called the local linearization of the system (38) around the equilibrium point $(x^{eq},\ u^{eq})$

On applying the above technique to our system defined by equation (33) (it should be noted that $y = g(x,u)$ is zero for our system. Therefore the C and D matrices are zero) around the equilibrium point defined by (37), we get,

$$A = \begin{bmatrix} 0 & 0 & 0 & 1 & 0 & 0 \\ 0 & 0 & 0 & 0 & 1 & 0 \\ 0 & 0 & 0 & 0 & 0 & 1 \\ -118.07 & -115.1993 & 0 & -38.5218 & 0 & 0.5872 \\ 55.0918 & 69.5758 & 0 & 15.4241 & 0 & -0.3546 \\ 3.9338 & 7.7940 & 0 & 0.6459 & 0 & -0.0897 \end{bmatrix} \quad (40)$$

$$B = \begin{bmatrix} 0 \\ 0 \\ 0 \\ 350.1986 \\ -140.2910 \\ -5.8715 \end{bmatrix}, \qquad C = \begin{bmatrix} 0 & 0 & 0 & 0 & 0 & 0 \end{bmatrix}, \qquad D = [0]$$

Now, for the LTI system defined by (39) to be stable, all the eigenvalues of A should lie on the left half of the complex plane. But, one the eigenvalues of A for our system lie on the imaginary axis and another one lies on the right side. Hence the system is unstable. But with the help of a feedback control law we can stabilize the system if it is controllable. To check for the existence of such a control law, we need to check the controllability of the system.

Theorem-2: A linear system defined by (38) is controllable if the controllability gramian defined as

$$CTRB := \begin{bmatrix} B & AB & A^2B & A^3B & \dots & A^{n-1}B \end{bmatrix} \quad (41)$$

has full rank.

But for our system, the controllability matrix has a rank of four. Hence the system is not completely controllable. But we can still use a feedback control law to stabilize the system around the equilibrium point if the uncontrollable states are stabilizable. There are different tests to find whether a system is stabilizable such as the Eigenvector test, Popov-Belevitch-Hautus (PBH) test, and the Lyapunov test. But, here, we use the controllability decomposition of the state space matrices (Kalman Decomposition for just controllability) and check for the stability of the uncontrollable states.

Theorem-3: From [18] for every LTI system of the form $\dot{x} = Ax + Bu$ can transformed through a similarity transform "T" into the standard form

$$\begin{bmatrix} \dot{x}_c \\ \dot{x}_{\bar{c}} \end{bmatrix} = \begin{bmatrix} A_c & A_{12} \\ 0 & A_{\bar{c}} \end{bmatrix} \begin{bmatrix} x_c \\ x_{\bar{c}} \end{bmatrix} + \begin{bmatrix} B_c \\ 0 \end{bmatrix} u \tag{42}$$

Where (A_c,B_c) is the controllable pair and the similarity transform "T" is defined as

$T := \begin{bmatrix} V_c & V_{\bar{c}} \end{bmatrix}$ where V_c forms a basis for the controllable subspace $\mathbb{C}$ defined as

$$\mathbb{C} = Im \begin{bmatrix} I_{\bar{n}x\bar{n}} \\ 0 \end{bmatrix}$$

of the pair (A,B).

Using the same eigenvalue test on the uncontrollable state matrix $A_{\bar{c}}$ we see that the eigenvalues are negative. That is the uncontrollable states are stable. Hence we can use linear feedback to control and stabilize the system around its equilibrium state.

3.4 Stability when $\beta_2 = 0$

The very same analysis was conducted when β_2 in equation (38) which corresponds to the friction between cart and ground is zero. We linearized the system around the equilibrium point and conducted the controllability test. Just like in the previous case, the controllability matrix had rank four. Hence we did controllability decomposition and eigenvalue analysis of uncontrollable modes. This stability analysis revealed that the system has uncontrollable modes with positive eigenvalues which means that the system is exploding and hence cannot be stabilized around the equilibrium point.

3.5 Stabilization around equilibrium point

In this work, we will be using a Linear Quadratic Regulator to stabilize the system. For a continuous linear time invariant system defined by the equation

$$\dot{x} = Ax + Bu,\ x \in \mathbb{R}^n,\ u \in \mathbb{R}^k,$$

Given a quadratic cost function defines as

$$J = x^T(t_1)F(t_1)x(t_1) + \int_{t_0}^{t_1}(x^TQx + u^TRu + 2x^TNu)dt \qquad (43)$$

the control law that minimizes the value of the cost function is

$$u(t) = -Kx(t) \qquad (44)$$

where $K = R^{-1}(B^TP + N^T)$

and P(t) is found by solving the algebraic Riccati differential equation

$$A^T P + PA - (PB + N)R^{-1}(B^T P + N^T) + Q = -\dot{P}(t) \quad (45)$$

with the boundary condition $P(t_1) = F(t_1)$ such that Q is a positive symmetric matrix, and $R > 0$.

In this work we use $Q = I_{6\times6}$ (where I is the identity matrix) and $R = 1$ to find the gain matrix K. Further, $P(t_1) = F(t_1) = 0$ and $N = [0]_{6\times6}$. Therefore, the cost function becomes,

$$J = \int_{t_0}^{\infty} (x^T Q x + u^T u) dt \quad (46)$$

The first term of the cost function J is the total path cost which is simply the sum of squares of the state variables and the second term is the energy cost which is just the square of the control input (since R=1). Integrating this over all the intervals, we get the total cost "J".

On solving the above equation we get

$$K = [-162.4701, -478.7420, -4.5312, -29.5405, -76.8044, -88.0402] \quad (47)$$

Substituting the above value of K in equation (44) we get the feedback control law that will stabilize the system. This control law minimizes the cost given by (46). Now, the closed loop system is given by

$$\begin{aligned} \dot{x} &= Ax + Bu \\ &= Ax + B(-Kx) \\ &= (A - BK)x \end{aligned} \quad (48)$$

The system given by equation (46) is the closed loop system. Now, to find the stability of the closed loop system, we can do the same eigenvalue test. As expected, the eigenvalues of the system $(A - BK)$ lie on the left half of the complex plane. Hence the closed loop system is stable and therefore any trajectory that starts within a δ neighborhood of the equilibrium will converge to $x^{eq}\ as\ t \to 0$.

It should also be noted that a regular pole placement technique using a feedback controller will also be able to stabilize the system. But finding an optimal gain value is very difficult using trial and error methods. Further, the position of the pole affects the dynamics a lot. If the poles are too far from the origin, the controller becomes very aggressive which might break the linearity assumption of the system and if it's too close to the origin, the controller might take a long time to reach the desired values.

Now we can go on to find the region of attraction of the LQR. The region of attraction (or domain of attraction) of the linear quadratic regulator is the set of points that can be brought to the desired equilibrium point using LQR. There are multiple ways to find the region of attraction such as using Lyapunov based sampling methods, and solving SOS equations. In Lyapunov based sampling methods[19], we solve the Lyapunov equation $A^T P + PA = -Q$ (where Q is a positive definite matrix) for P, find the Lyapunov function candidate $V(x) = x^T Px$, find $\dot{V}(x)$ find c^* and sublevel set $V(c^*)$ defined as

$$V(c^{*}) = \{x \in X : V(x) \leq c^{*}\},\ x \in \mathbb{R}^{n} \quad (49)$$

is the domain of attraction. It should also be noted that if P is positive definite then the system is stable. In the SOS method we try to optimize a SOS problem to find the region of convergence for the system. In this work,we find the region of attraction by using a completely numerical method. For a set of initial conditions, we check whether the feedback LQR controller is able to take the system ϵ close to the equilibrium in finite time. The set of points which satisfy the above condition is part of the region of attraction of the LQR.

3.6 Results.

The system was initialized with the following initial condition.

$$x_0 = [-0.9860, 0.0200, -0.1049, -0.4290, 2.4184, 0.7098]$$

The figures below describe the dynamics of the system, the total energy of the system and the value of the control input.

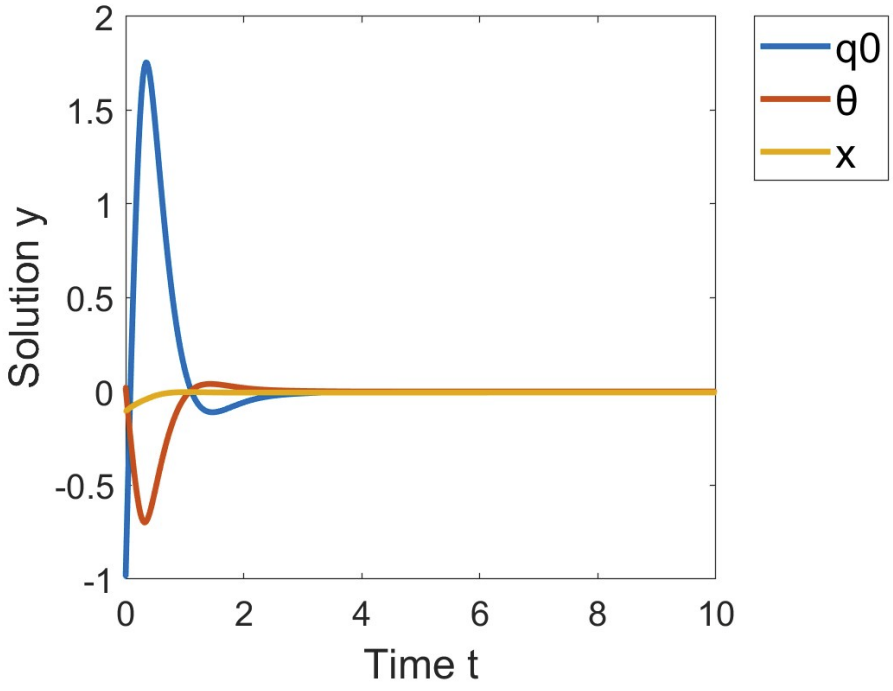

Figure: 3.1 Dynamics converging to the equilibrium point using LQR

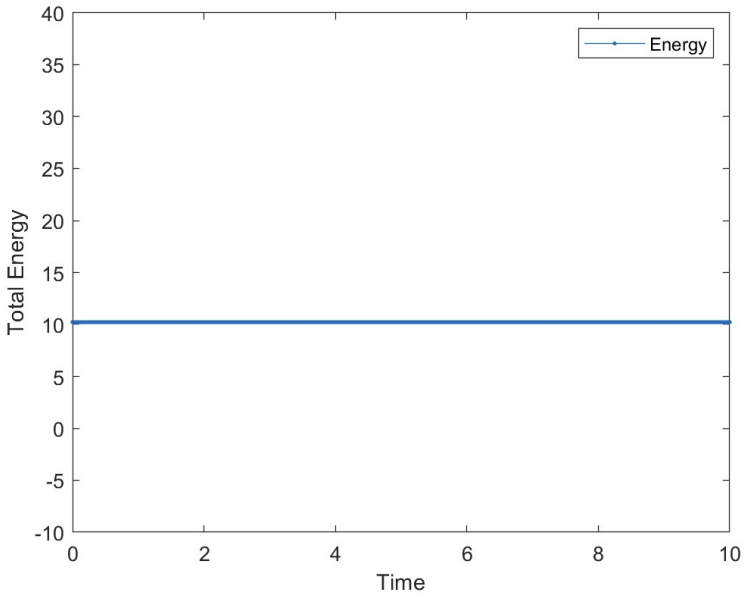

Figure: 3.2 Total energy of the system starting from x_0

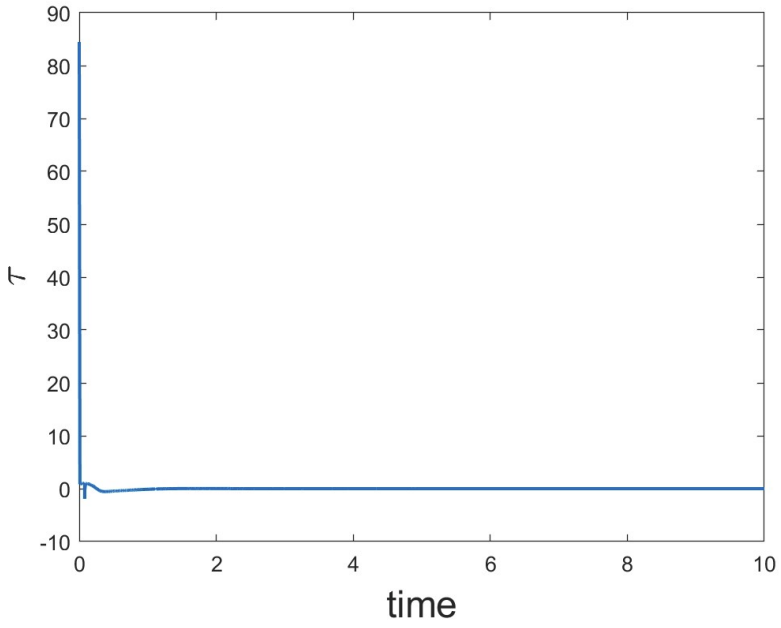

Figure: 3.3 Value of the control input τ_1

3.7 Actuating the curvature vs actuating the cart position

Now, the same procedure was repeated for the system, but this time, instead of actuating the curvature, the acceleration of the cart was actuated. It was found experimentally that for stiffness, $k < 0.55$, the system does not converge to the equilibrium point. Therefore, the control input of the two system where compared with $k = 0.55$. It should be noted the both systems where controllable for $k = 0.55$. The dynamics, energy and control values of the system are given in figures 3.4, 3.5 and 3.6. Both the systems were initiated close to the origin with initial value,

$x_0 = [0.01,\ 0,\ 0,\ 0,\ 0,\ 0]$. The energy of the system in the upright position is 9.8J. It can bee seen from the figures that the system converges to the equilibrium point faster when $\ddot{q}_0$ is actuated.

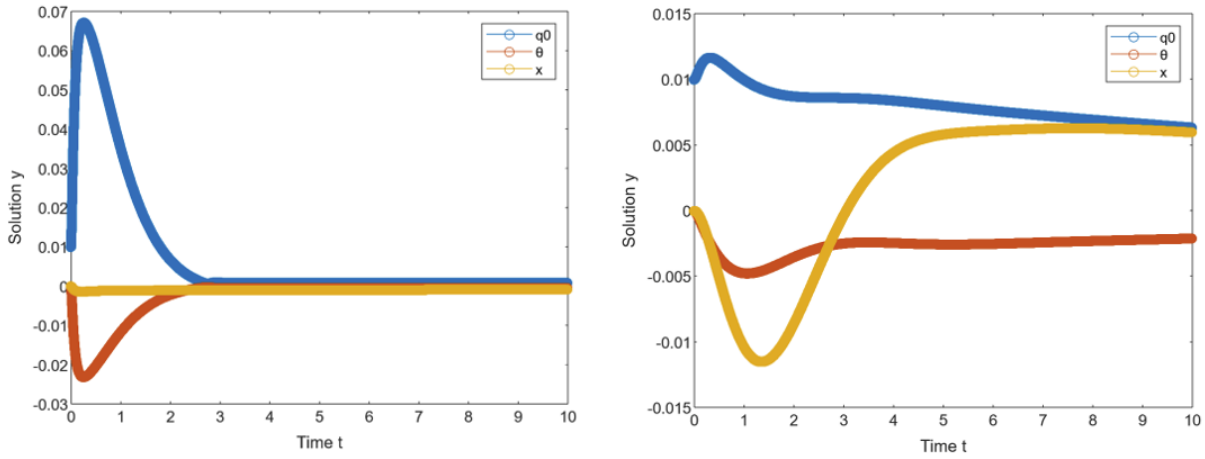

Figure: 3.4 Dynamics of the system. actuated $\ddot{q}_0$ on the left and $\ddot{x}_p$ on the right

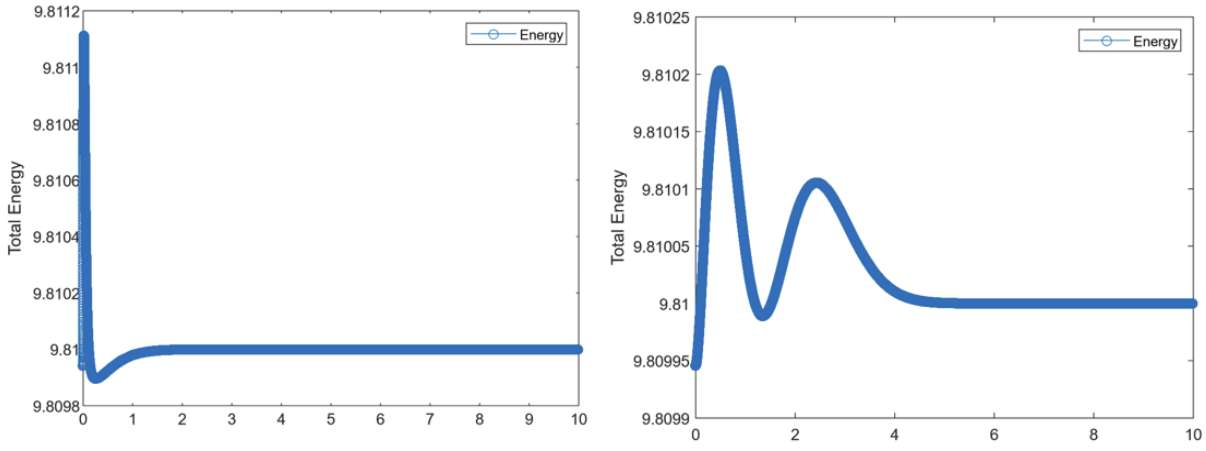

Figure: 3.5 Energies of the system. actuated $\ddot{q}_0$ on the left and $\ddot{x}_p$ on the right

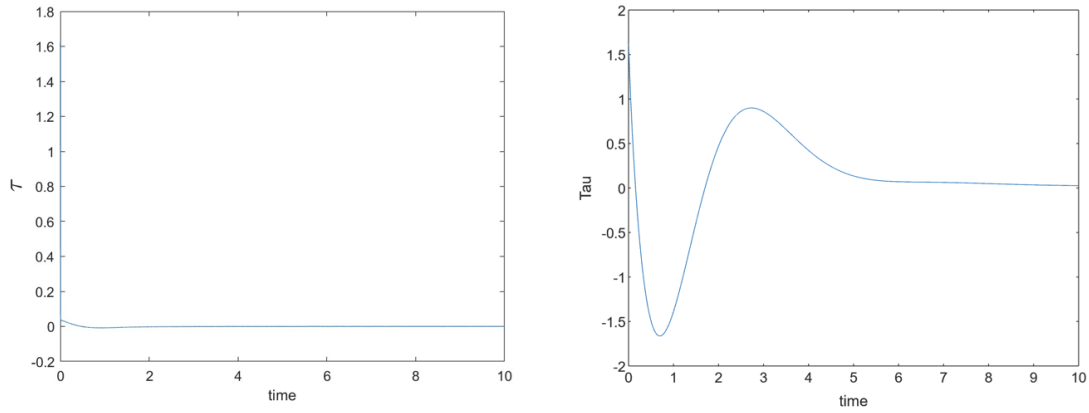

Figure: 3.6 Control inputs of the system. actuated $\ddot{q}_0$ on the left and $\ddot{x}_p$ on the right

The convergence of the system for $k = 10,\ k = 5\ and\ k = 3$ are shown below.

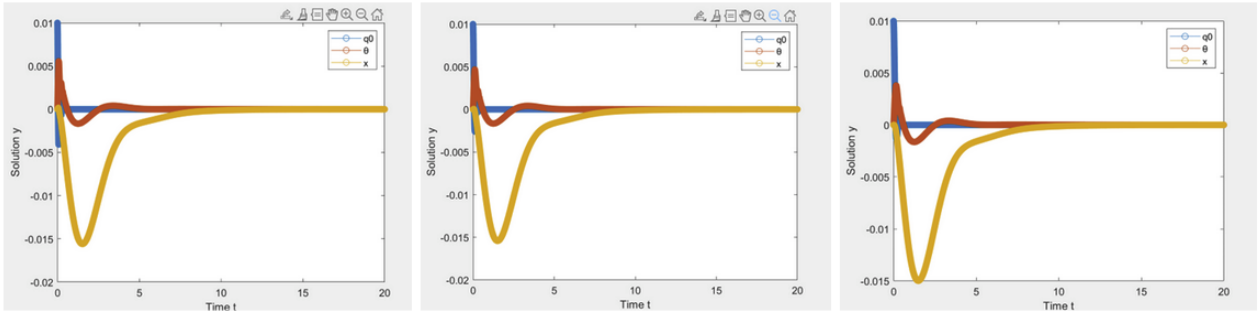

Figure: 3.7 Convergence of system for values of $k = 10,\ k = 5\ and\ k = 3$

3.8 Summary

In this chapter we discussed the nature of equilibrium points, regarding the controllability of the system, linearization, feedback control law and linear quadratic regulator. We used controllability decomposition to check whether the system is stabilizable, and used both pole placement technique and LQR to

stabilize the system. Experiments revealed that as expected, LQR gives better results in terms of total energy and better dynamics.

Chapter-4 Swing-up Design

4.1 Introduction

In this chapter we develop the swing up control for the system, derive the necessary conditions for the swing up control to work, stability analysis of the obtained control law, and the robustness of the controller. Swing-up control of under-actuated systems like acrobot, pendubot and double pendulum has been a field of study for a long time. Swing-up control of an acrobot using an energy based method is discussed in detail in [25] while the control using partial-feedback linearization is detailed in [7]. In [13] it has been successfully shown that the same energy based control with modifications in Lyapunov function candidate can be used for pendubot. A passivity based control strategy was successfully developed for inverted-pendulum-system in [26]. Further, in [23] a double-pendulum on a cart was successfully stabilized at the vertical equilibrium using energy based-swing-up and LQR control. In addition, modern sample based control methods such as Monte Carlo Model Predictive Control [27] has been successfully employed for the swing-up control of inverted pendulum on a cart.

In this work, we have used an energy based method for the swing-up control of the SIPC system. For this, we use a Lyapunov function based method to derive the control law. For this, first we need to derive the total energy of the system. Then, we formulate an energy based general Lyapunov function and derive the control input from this. We will also find the homoclinic orbit and prove that the derived

control law will take you from any initial point in the state space to the homoclinic orbit. For this, we will use LaSalle's invariance principle. The system is in homoclinic orbit when the total energy of the system is equal to the energy of the system when it is in upright condition with predetermined conditions satisfied. Once the system is in the homoclinic orbit, we can use the linear quadratic regulator that we designed in the previous chapter to stabilize the system once the pendulum reaches within the LQR's region of attraction.

4.2 Energy of the System

First we will find the total energy of the system.

From the previous chapters, first we calculate the sum of kinetic energy and potential energy of the system. The total kinetic energy is given by

$$KE = \frac{1}{2}\dot{q}^{T} D(q)\, \dot{q}$$

where D(q) is the inertia matrix and $\dot{q} = \left[\dot{q}_0(t),\ \dot{\theta}(t),\ \dot{x}_p(t)\right]$ and the total potential energy is given by

$$PE = -\frac{Lgm_p cos(q_0 + \theta) - Lgm_p cos(\theta) + Lq_0 gm_p sin(\theta)}{q_0^2}$$

But, since we have damping and stiffness terms, we need to take these terms also into consideration

This will be contributed by

$$Eg = \frac{1}{2} q^{T} K_k q \qquad (50)$$

where K_k is the matrix introduced in chapter two and $q = \left[q_0(t),\ \theta(t),\ x_p(t)\right]$

Therefore total energy

$$E = KE + PE + Eg \tag{51}$$

$$= \frac{1}{2}\dot{q}^{T} D(q)\,\dot{q} - \frac{Lgm_p cos(q_0 + \theta) - Lgm_p cos(\theta) + Lq_0 gm_p sin(\theta)}{q_0^2} + \frac{1}{2}q^{T} K_k q$$

$$= \frac{1}{2}\dot{q}^{T} D(q)\,\dot{q} - \frac{Lgm_p cos(q_0 + \theta) - Lgm_p cos(\theta) + Lq_0 gm_p sin(\theta)}{q_0^2} + \frac{1}{2}kq_0^2 \tag{52}$$

Now, differentiating total energy E wrt time we get,

$$\dot{E} = \dot{q}^{T} D(q)\,\ddot{q} + \frac{1}{2}\dot{q}^{T}\dot{D}\dot{q} + \dot{q}^{T} K_k q + \dot{PE} \tag{53}$$

Now,

$$\dot{PE} = \frac{dPE}{dt} = \frac{dPE}{dq}\frac{dq}{dt} = \dot{q}^{T} G \tag{54}$$

where $G = \frac{dPE}{dq}$

Substituting equation (54) back in (53) we get,

$$\dot{E} = \dot{q}^{T} D(q)\,\ddot{q} + \frac{1}{2}\dot{q}^{T}\dot{D}\dot{q} + \dot{q}^{T} K_k q + \dot{q}^{T} G \tag{55}$$

But from chapter two we know

$$D(q)\,\ddot{q}(t) + C(q,\dot{q})\dot{q} + B_\beta \dot{q} + K_k q + G(q) = \tau$$

$$\Downarrow$$

$$D(q)\,\ddot{q}(t) = \tau - (C(q,\dot{q})\dot{q} + B_\beta \dot{q} + K_k q + G(q)) \tag{56}$$

Substituting (56) in (55) we get,

$$\dot{E} = \dot{q}^{T}(\tau - (C(q,\dot{q})\dot{q} + B_{\beta}\dot{q} + K_{k}q + G(q))) + \frac{1}{2}\dot{q}^{T}\dot{D}\dot{q} + \dot{q}^{T}K_{k}q + \dot{q}^{T}G$$

$$= \dot{q}^{T}\tau - \dot{q}^{T}C(q,\dot{q})\dot{q} - \dot{q}^{T}B_{\beta}\dot{q} - \dot{q}^{T}K_{k}q - \dot{q}^{T}G(q) + \frac{1}{2}\dot{q}^{T}\dot{D}\dot{q} + \dot{q}^{T}K_{k}q + \dot{q}^{T}G$$

$$= \dot{q}^{T}\tau - \dot{q}^{T}C(q,\dot{q})\dot{q} - \dot{q}^{T}B_{\beta}\dot{q} + \frac{1}{2}\dot{q}^{T}\dot{D}\dot{q} \quad (57)$$

But we know

$$\tau = \begin{bmatrix}\tau_1\\ \tau_2\\ \tau_3\end{bmatrix} = \begin{bmatrix}\tau_1\\ 0\\ 0\end{bmatrix} \quad (58)$$

Substituting this in (57) and simplifying we get,

$$\dot{E} = \dot{q}^{T}\tau - \dot{q}^{T}C(q,\dot{q})\dot{q} - \dot{q}^{T}B_{\beta}\dot{q} + \frac{1}{2}\dot{q}^{T}\dot{D}\dot{q}$$

$$= \dot{q}_{0}\tau_{1} - \dot{q}^{T}C(q,\dot{q})\dot{q} - \dot{q}^{T}B_{\beta}\dot{q} + \frac{1}{2}\dot{q}^{T}\dot{D}\dot{q} \quad (59)$$

Now, from properties of the inertia matrix D and coriolis and centrifugal matrix C we know that the matrix $\dot{D} - 2C$ is skew-symmetric.

If a matrix H_{nxn} is skew-symmetric then

$$a^{T}Ha = 0,\ a \in \mathbb{R}^{1\times n} \quad (60)$$

Using the above property since $\dot{M} - 2C$ is skew-symmetric,

$$q^{T}(\dot{M} - 2C)q = 0 \text{ since } q \in \mathbb{R}^{1\times 6} \quad (61)$$

Therefore,

$$\dot{E} = \dot{q}_0 \tau_1 - \dot{q}^T C(q,\dot{q})\dot{q} - \dot{q}^T B_\beta \dot{q} + \frac{1}{2}\dot{q}^T \dot{D}\dot{q}$$

$$= \dot{q}_0 \tau_1 + \frac{1}{2}\dot{q}^T (\dot{D} - 2C(q,\dot{q}))\dot{q} - \dot{q}^T B_\beta \dot{q}$$

$$= \dot{q}_0 \tau_1 - \dot{q}^T B_\beta \dot{q} \quad (62)$$

We know

$$B_\beta = \begin{bmatrix} \beta_1 & 0 & 0 \\ 0 & 0 & 0 \\ 0 & 0 & \beta_2 \end{bmatrix}$$

Substituting this in 62 we get,

$$\dot{E} = \dot{q}_0 \tau_1 - (\beta_1 \dot{q}_0^2 + \beta_2 \dot{x}_p^2) \quad (63)$$

Now we want to find a control law which takes the system from any initial point to the homoclinic orbit. Now, to find the homoclinic orbit, we find the total energy of the system in the upright position. The total energy of the system in upright position is the sum of energies of the pendulum and cart. Since the cart is always on the ground, the energy of the cart should be zero. Therefore, the energy of the system is just the energy of the pendulum which is defined as $\overline{E}$. When the pendulum is in upright position, $q_0 = 0$ and $\dot{q}_0 = 0$ Substituting this in total energy equation we get,

$$\overline{E} = \frac{m_p * g * L}{2} \quad (64)$$

4.3 Homoclinic Orbit

From [17] we define homoclinic orbit.

Consider the system

$$\dot{x} = f(x).$$

Suppose that there exists an equilibrium point x_0. Then the solution of the system $\varphi(x)$ is homoclinic if

$$\varphi(x) \to x_0 \text{ as } t \to \infty$$

For our system, homoclinic orbit is characterized by a set of points such that

- $E(x) = \overline{E}(x)$
- $q_0 = 0$ (64)
- $\dot{q}_0 = 0$

Substituting for q_0 and $\dot{q}_0$ in equation (52) we get,

$$E = \frac{(m_c+m_p)(\dot{x}_p)^2}{2} - \frac{Lm_p cos(\theta)\dot{\theta}}{4} + \frac{m_p(4L^2+D^2)(\dot{\theta})^2}{24} - \frac{Lm_p cos(\theta)(\dot{x}_p)(\dot{\theta})}{4} + \frac{Lm_p gcos(\theta)}{2}$$

(65)

$$E = \frac{(m_c+m_p)(\dot{x}_p)^2}{2} + \dot{\theta}\left[\frac{-6Lm_p cos(\theta)+m_p(4L^2+D^2)(\dot{\theta}) \ -6Lm_p cos(\theta)\dot{x}_p}{24}\right] + \frac{Lm_p gcos(\theta)}{2}$$

(66)

Equating $E(x) = \overline{E}(x) = \frac{m^*g^*L}{2}$ we get

$$\frac{(m_c+m_p)(\dot{x}_p)^2}{2} + \dot{\theta}\left[\frac{-6Lm_p cos(\theta)+m_p(4L^2+D^2)(\dot{\theta})\ -6Lm_p cos(\theta)\dot{x}_p}{24}\right] + \frac{Lm_p gcos(\theta)}{2} - \frac{m_p gL}{2} = 0$$

(67)

which is the homoclinic orbit. Now the control law that we drive should take the system to this homoclinic orbit.

4.4 Control Law

Now, we need a Lyapunov Function V(x). Following the steps in [4] and [11] we define the Lyapunov function

$$V(q,\dot{q}) = \frac{k_e}{2}(E - \bar{E})^2 + \frac{k_d}{2}\dot{q}_0^2 + \frac{k_p}{2}q_0^2 \tag{68}$$

such that $k_p,\ k_d,\ k_e > 0$ Now we need to calculate the derivative of this Lyapunov function candidate along the trajectories of the state equation.

$$\dot{V}(q,\dot{q}) = k_e(E - \bar{E})\,\dot{E} + k_d\dot{q}_0\ddot{q}_0 + k_p\dot{q}_0 q_0 \tag{69}$$

Now, we substitute $\dot{E}$ from equation (63) to the above equation we get,

$$\dot{V}(q,\dot{q}) = k_e(E - \bar{E})\,(\dot{q}_0\,\tau_1 - (\beta_1\dot{q}_0^2 + \beta_2\dot{x}_p^2)) + k_d\dot{q}_0\ddot{q}_0 + k_p\dot{q}_0 q_0 \tag{70}$$

$$= \dot{q}_0\,(k_e(E - \bar{E})(\tau_1 - \beta_1\dot{q}_0) + k_d\ddot{q}_0 + k_p q_0) - k_e(E - \bar{E})\beta_2\dot{x}_p^2 \tag{71}$$

$$= \dot{q}_0\,(k_e(E - \bar{E})(\tau_1 - \beta_1\dot{q}_0 - \frac{\beta_2\dot{x}_p^2}{\dot{q}_0}) + k_d\ddot{q}_0 + k_p q_0)$$

Now, we want $\dot{V}(q,\dot{q})$ to be negative. For this, if we make

$$-\dot{q_0} = (k_e(E - \overline{E})(\tau_1 - \beta_1\dot{q_0} - \frac{\beta_2\dot{x_p}^2}{\dot{q_0}}) + k_d\ddot{q_0} + k_p q_0) \quad (72)$$

Then,

$$\dot{V}(q,\dot{q}) = \dot{q_0} * (-\dot{q_0})$$

In the next sections we find k_e, k_p, k_d such that the control input τ_1 is stable.

$$\dot{V}(q,\dot{q}) = \dot{q_0} * (-\dot{q_0}) = -\dot{q_0}^2 \leq 0$$

which implies that,

$$\dot{V}(q,\dot{q}) \leq 0$$

Therefore we can go on to derive the control input required for the system from the above expressions..

Now, from the dynamics discussed in earlier chapters, the state dynamics can be written as

$$\ddot{q_0} = f_{11}\tau_1 + f_{12} \quad (73)$$

$$\ddot{\theta} = f_{22} \quad (74)$$

$$\ddot{x_p} = f_{32} \quad (75)$$

Substituting this in equation (71) we get,

$$-\dot{q_0} = (k_e(E - \overline{E})(\tau_1 - \beta_1\dot{q_0} - \frac{\beta_2\dot{x_p}^2}{\dot{q_0}}) + k_d(f_{11}\tau_1 + f_{12}) + k_p q_0)$$

$$= \tau_1(k_e(E - \overline{E}) + k_d f_{11}) + (-k_e(E - \overline{E})(\beta_1\dot{q_0} + \frac{\beta_2\dot{x_p}^2}{\dot{q_0}}) + k_d f_{12} + k_p q_0)$$

(76)

From the above expression we get,

$$\tau_1(k_e(E - \overline{E}) + k_d f_{11}) = -\dot{q}_0 + k_e(E - \overline{E})(\beta_1 \dot{q}_0 + \frac{\beta_2 \dot{x}_p^2}{\dot{q}_0}) + k_d f_{12} + k_p q_0$$

(77)

Finally, we get,

$$\tau_1 = \frac{-\dot{q}_0 + (k_e(E-\overline{E})(\beta_1 \dot{q}_0 + \frac{\beta_2 \dot{x}_p^2}{\dot{q}_0}) - k_d f_{12} - k_p q_0)}{k_e(E-\overline{E}) + k_d f_{11}} \quad (78)$$

$$\tau_1 = \frac{-\dot{q}_0 + (k_e \widehat{E}(-\beta_1 \dot{q}_0 + \frac{\beta_2 \dot{x}_p^2}{\dot{q}_0}) - k_d f_{12} - k_p q_0)}{k_e \widehat{E} + k_d f_{11}} \quad (79)$$

where $\widehat{E} = E - \overline{E}$ is the error in energy between the final energy and the instantaneous energy.

4.5 Stability analysis of Control Law

This control input should be able to take the system from any arbitrary initial point to the homoclinic orbit defined by (66). In the subsequent section we will prove the stability of the control input and derive the necessary condition that the control input τ_1 should satisfy.

If the term

$$\dot{q}_0(k_e(E - \overline{E}) + k_d f_{11}) \neq 0 \quad (80)$$

in the denominator of the control input is not zero, then the expression won't have any singularities.

First, let us consider the case where,

$$k_e\widehat{E} + k_d f_{11} \neq 0$$

From the above expression we can write,

$$|\widehat{E}| < \frac{k_d f_{11}}{k_e} \tag{81}$$

because f_{11} is an element of D(q) which is bounded. Therefore each element of the matrix is bounded.

Therefore, the above condition will be satisfied for some $\delta > 0$

$$|\widehat{E}| \leq (\frac{k_d}{k_e} - \delta) f_{11} < \frac{k_d f_{11}}{k_e} \tag{82}$$

Now for the above control law, we need to avoid getting stuck at the stable equilibrium point which is the bottom one. To do this we first find the energy of the pendulum when it is in the stable equilibrium point. We can directly find this by substituting $\theta = \pi$ in the potential energy equation. Following this we get

$$E_{bottom} = -\frac{m_p g L}{2} \tag{83}$$

In order to achieve this we need

$$|\widehat{E}| < m_p g L \tag{84}$$

Therefore, taking equation (80) and (82) into account, we get,

$$|\widehat{E}| < min(m_p gL, (\frac{k_d}{k_e} - \delta) f_{11}) = c$$

(85)

$$|\widehat{E}| < c$$

where,

$$c = min(m_p gL, (\frac{k_d}{k_e} - \delta) f_{11})$$

Since we know that $\dot{V}(q, \dot{q}) \leq 0$, $V(q, \dot{q})$ is a decreasing function. Therefore the maximum value of $V(q, \dot{q})$ will be the initial condition itself. Hence the above equation will hold if

$$V(0) < \frac{c^2}{2} \tag{86}$$

Further, from equation (80), the system will have singularities if $\dot{q}_0 = 0$. Therefore, the system cannot be initialized with $\dot{q}_0 = 0$. Combining this two, the region defined by $\left\{x: V(x) < \frac{c^2}{2} \cap \dot{q}_0 \neq 0\right\}$ is the region of attraction of the swing up control. If the initial points are inside this, then the controller will be able to take the system to the homoclinic orbit.

Now we use LaSalle's invariance theorem to discuss the stability of the control input.

From [17] LaSalle's invariance theorem says that, let $\Omega \subset D$ be a compact set that is positively invariant with respect to

$$\dot{x} = f(x)$$

Let V: $D \to R$ be a continuously differentiable function such that $\dot{V}(x) < 0$ in Ω. Let E be the set of all points in Ω where $\dot{V}(x) = 0$. Let M be the largest invariant set in E. Then every solution starting in Ω approaches M as $t \to \infty$,

For our system, we know, $\dot{V}(q, \dot{q}) = -\dot{q}_0^{\,2}$ which is always less than or equal to zero since $\dot{q}_0 \in \mathbb{R}^1$. This means that $V(q, \dot{q})$ is non increasing. Therefore $\left[q_0(t),\ \theta(t),\ x_p(t),\ \dot{q}_0(t),\ \dot{\theta}(t),\ \dot{x}_p(t)\right]$ are bounded. Further, from the above analysis, the error in energy $\widehat{E}$ is bounded. Now, let Ω be the compact set of the system defined by (27) that is positively invariant (which means every solution that starts in Ω stays in Ω for all future time). Let Ψ be the set of all points in Ω such that $\dot{V}(x) \equiv 0$. i.e.,

$$\Psi = \left\{q_0(t),\ \theta(t),\ x_p(t),\ \dot{q}_0(t),\ \dot{\theta}(t),\ \dot{x}_p(t)\right\}: \dot{V}(q, \dot{q}) \equiv 0$$

Let $M \in \Psi$ be the largest invariant set in Ψ. Then from LaSalle's invariance principle all solution starting in Ω approaches M as $t \to \infty$. Now we will find this largest invariant set M in Ω. For the set Ψ, $\dot{V}(q, \dot{q}) \equiv 0$ which implies that $-\dot{q}_0^{\,2} = 0 \Rightarrow \dot{q}_0 = 0$ which means that q_0 is a constant. Further, since $\dot{q}_0 = 0$, $\ddot{q}_0 = 0$. Now $\dot{V}(q, \dot{q}) \equiv 0$ also implies that $V(q, \dot{q})$ is a constant which means from equation (67)

$$\frac{k_e}{2}(E - \overline{E})^2 + \frac{k_d}{2}\dot{q}_0^2 + \frac{k_p}{2}q_0^2 = constant \quad (87)$$

Since k_e, k_p, and k_d are constants and $\dot{q}_0 = 0$ and q_0 is a constant, $\widehat{E}^2 = (E - \overline{E})^2$ is also a constant which means $\widehat{E}$ is also a constant. Therefore $\widehat{E} = 0$ or $\widehat{E} \neq 0$.

We know from the above discussion that

$$-\dot{q}_0 = (k_e\widehat{E}(\tau_1 - \beta_1\dot{q}_0 - \frac{\beta_2\dot{x}_p^2}{\dot{q}_0}) + k_d\ddot{q}_0 + k_p q_0)$$

Substituting $\ddot{q}_0 = 0$ and taking the limit when $\dot{q}_0 = 0$, in the above equation we get,

$$k_e\widehat{E}\tau_1 + k_p q_0 = 0 \quad (88)$$

First, let us consider the case when $\widehat{E} = 0$. When $\widehat{E} = 0$, from the above equation $q_0 = 0$. These are the conditions defined by equations (64) which we used for defining the homoclinic orbit and hence the trajectory belongs to the homoclinic orbit.

Now let us consider the case when $\widehat{E} \neq 0$ but is a constant. From equation (87), since k_e, k_p, q_0 and $\widehat{E}$ are constants, τ_1 should also be a constant. Also from (69) when $\dot{q} = 0$ we get $V(q, \dot{q}) = \frac{k_e}{2}\widehat{E}^2 + \frac{k_p}{2}q_0^2$. We know from the above discussion that $V(q, \dot{q})$ is non- decreasing which means that

$$V(q, \dot{q}) = \frac{k_e}{2}\widehat{E}^2 + \frac{k_p}{2}q_0^2 \leq V(0) \quad (89)$$

From the above equation, since both $\widehat{E}^2$ and q_0^2 are positive we can write

$$\frac{k_p}{2}q_0^2 \leq V(q,\dot{q}) \leq V(0) \Rightarrow \frac{k_p}{2}q_0^2 \leq V(0)$$

$$\frac{k_p}{2}q_0^2 \leq V(0) \Rightarrow \sqrt{k_p}|q_0| \leq \sqrt{2V(0)} \quad (90)$$

From (87) we get $k_e\widehat{E}\tau_1 = -k_p q_0 = \sqrt{k_p}\sqrt{k_p}q_0$. Taking the absolute value on both sides we get,

$$k_e|\widehat{E}\tau_1| = \sqrt{k_p}\sqrt{k_p}|q_0| \quad (91)$$

Substituting (89) in (90) we get,

$$k_e|\widehat{E}\tau_1| = \sqrt{k_p}\sqrt{k_p}|q_0| \leq \sqrt{k_p}\sqrt{2V(0)} \quad (92)$$

Now substituting from (86) we get,

$$k_e|\widehat{E}\tau_1| \leq \sqrt{k_p}c$$

Which means $$|\widehat{E}\tau_1| \leq \frac{\sqrt{k_p}c}{k_e} \quad (93)$$

From equation (93) we can see that for appropriate values of k_e *and* k_p, $|\widehat{E}\tau_1|$ will be a small value which means, since $\widehat{E}$ is bounded, τ_1 will also be bounded and will be small.

Since $\dot{q_0} \equiv 0$, q_0 is a constant. When it comes to the rate of base rotation $\dot{\theta}$ and velocity of the cart $\dot{x_p}$, it could be zero or not. Considering $\dot{\theta} \neq 0$ means that θ is continuously changing. If $\dot{\theta} \neq 0$, the rotation will result in a gravity induced

torque on the soft robot's body which will cause it to change its degree of curvature which means $\dot{q_0} \neq 0$. But this is a contradiction against our assumption that $\dot{q_0} \equiv 0$ and hence is not possible. Therefore $\dot{\theta} = 0$. Now if $\dot{x_p} \neq 0$, then the gravity induced force (reaction force) will cause a change in the angle θ which means that $\dot{\theta} \neq 0$ which in turn means that $\dot{q_0} \neq 0$ which is again a contradiction. Hence $\dot{x_p} = 0$.

Also, the curvature and base rotation are constants only if τ_1 is exactly compensating gravity and stiffness induced torque. From the above derivation we know that τ_1 is small which is only possible if q_0 is close to zero. Otherwise τ_1 will be large so as to bring q_0 close to zero. Therefore q_0 has to be close to zero. Therefore, for τ_1 to be close to zero θ should be close to zero or θ should be close to π ($\theta \simeq 0 \; or \; \theta \simeq \pi$). But $\theta \simeq \pi$ is excluded since its not the desired equilibrium which means that $\theta \simeq 0$. Therefore, $|q_0| < \varepsilon_*$ and $|\theta| < \varepsilon_*$ where ε_* is an arbitrarily small constant. In addition to this, if we substitute the conditions $\tau = 0,\ q_0 = 0,\ \dot{q_0} = 0,\ \ddot{q_0} = 0,\ \dot{x_p} = 0$, $\dot{\theta} = 0$ and $\ddot{\theta} = 0$ in the equation

$$\ddot{q(t)} = D(q)^{-1}(\tau - (C(q,\dot{q})\dot{q} + B_\beta \dot{q} + K_k q + G(q)))$$

we get $\theta \equiv 0$. Therefore the largest invariant set Q in Ψ is given by the set of points in the homoclinic orbit and the interval

$\left(q_0,\ \theta,\ x_p,\ \dot{q}_0,\ \dot{\theta},\ \dot{x}_p\right) = (\varepsilon,\ 0,\ x_p,\ \varepsilon,\ 0,\ 0)$ where $|\varepsilon| < \varepsilon_*$. Therefore finally the largest invariant set M in ψ is defined as,

$$M = \left\{\left(q_0,\ \theta,\ x_p,\ \dot{q}_0,\ \dot{\theta},\ \dot{x}_p\right):\ q_0 \equiv 0,\ \dot{q}_0 \equiv 0,\ and\ satisfies\ equation\ (67)\right\}$$

$$\bigcup \left\{\left(q_0,\ \theta,\ x_p,\ \dot{q}_0,\ \dot{\theta},\ \dot{x}_p\right), \left(q_0,\ \theta,\ x_p,\ \dot{q}_0,\ \dot{\theta},\ \dot{x}_p\right) = (\varepsilon,\ 0,\ x_p,\ \varepsilon,\ 0,\ 0), |\varepsilon| < \varepsilon_*\right\} \tag{94}$$

It should be noted that even though the control input has a division by $\dot{q}_0$, during simulation, this never caused an issue.

4.6 Results

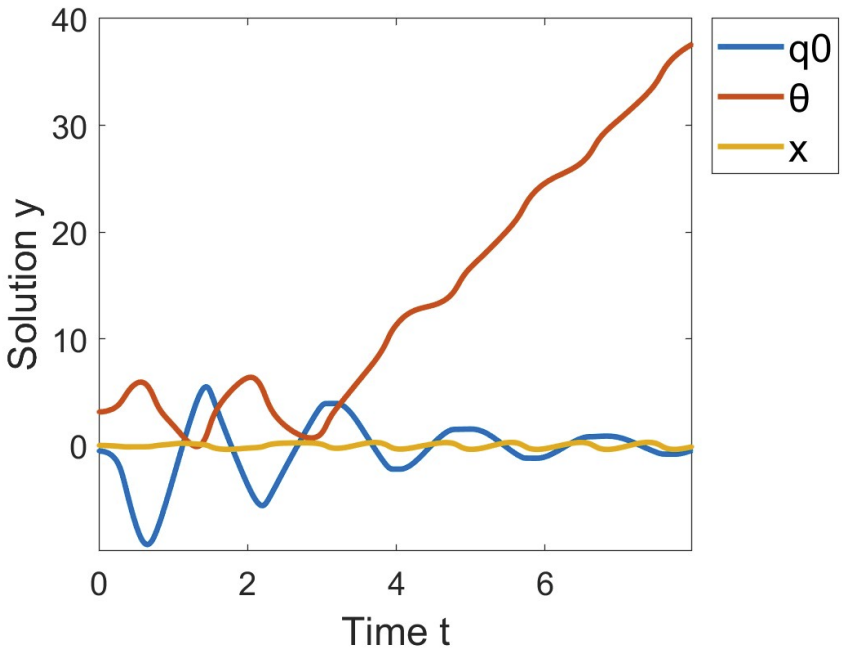

Figure: 4.1 Swing-up control

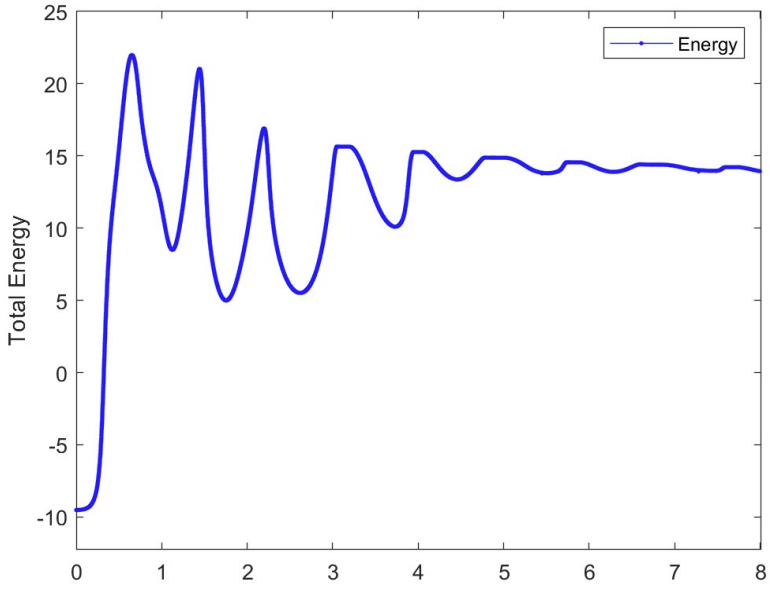

Figure: 4.2 Total energy of the system during Swing-up control

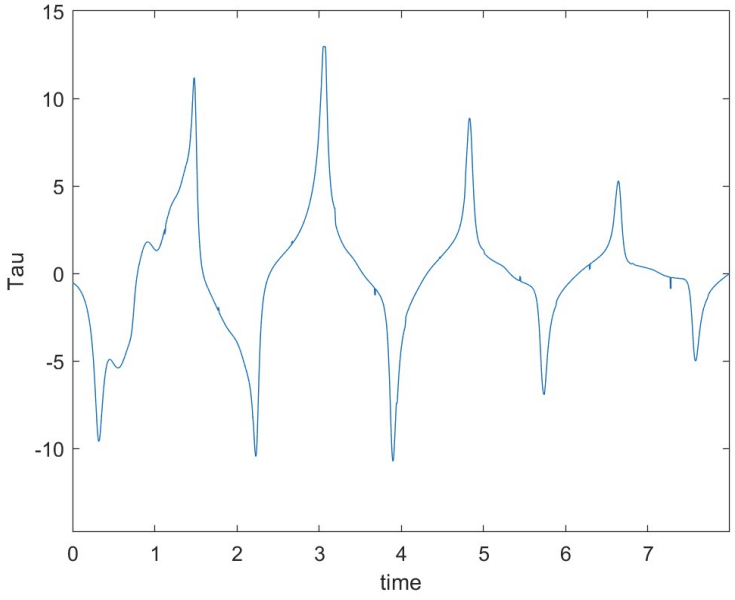

Figure: 4.3 Control input

The swing-up control of the system starting from the initial point $x_0 = [-\frac{\pi}{6}, \pi, 0, 0.001, 0, 0]$ is given above. As we can see from figure 4.2, the system has not reached the homoclinic orbit yet (the total energy of the system

is not 9.8J). In figure: 4.10 we can see that the system initialized from the same point has reached homoclinic orbit at around 15 seconds and has switched to LQR at around 16 seconds.

The swing-up control and stabilization of the system starting from the vertically down position with the cart at the origin ($x_p = 0$) is given below. The system is switched to LQR at around 16.5 seconds (system is within the region of attraction of LQR). You can notice a sudden jump in the value of theta. Note that we derived the LQR for the reference value $x_0 = [0, 0, 0, 0, 0, 0]$. Therefore to check whether the system is within the region of attraction and to initialize the LQR, we divide θ by 2π and take the remainder. This doesn't make any difference to the system dynamics because, for the pendulum, the rotation $2n\pi \pm \nu$ from the vertical is same as $\pm\ \nu$ (since 2π is one complete rotation).

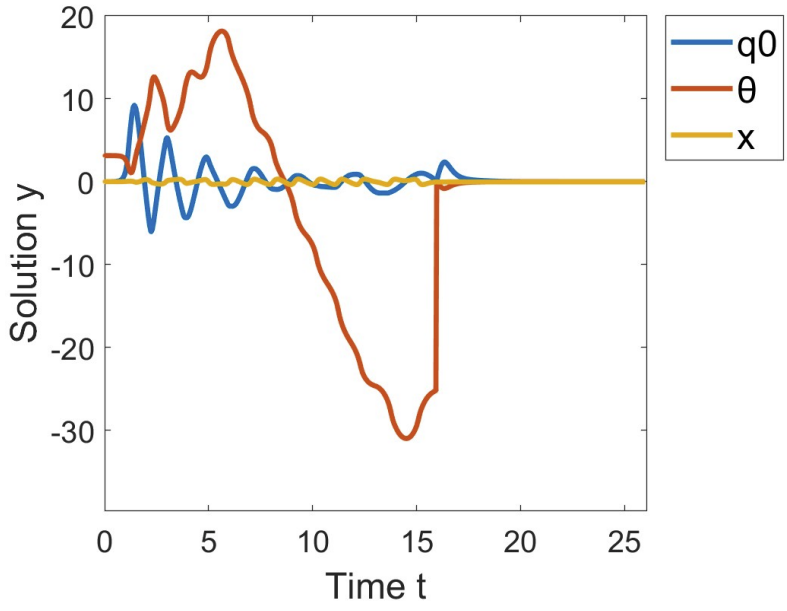

Figure: 4.4 Swing-up control and stabilization

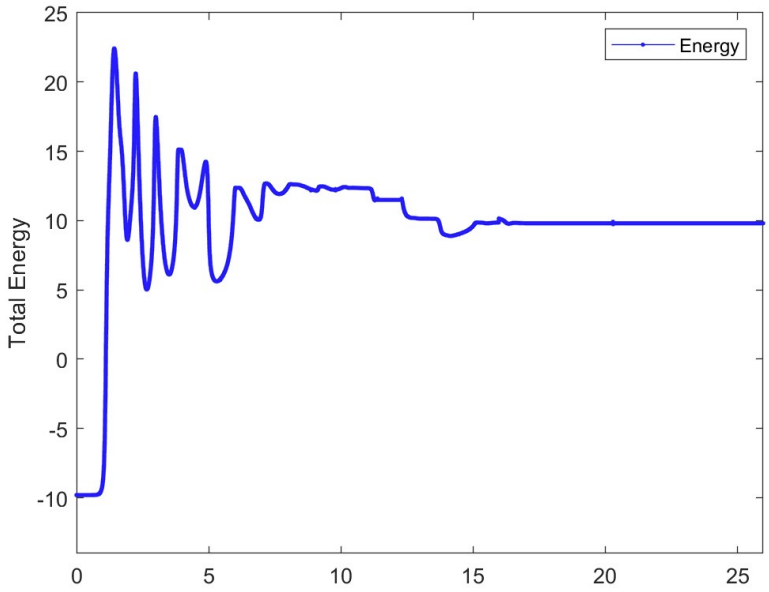

Figure: 4.5 Energy of the system

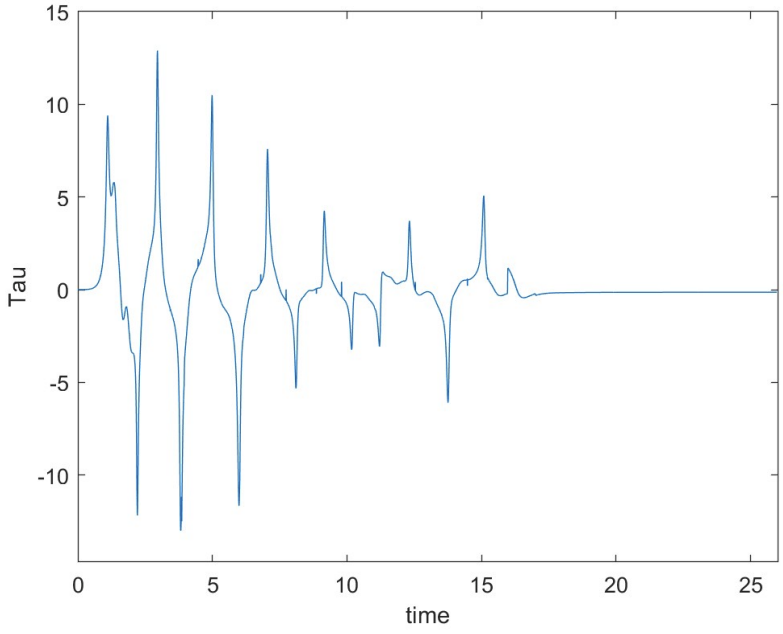

Figure: 4.6 Control input

The swing-up control of the system starting from the vertically down position with the cart at $x_p = 10$ ($x_0 = [0.001, \pi, 10, 0.001, 0, 0]$) is given below. Just like in the first case, the system is switched to LQR starting at around twenty two seconds when the system is inside the region of attraction of the LQR. Just as in the previous case, you can see a sudden jump in the value of θ. We can notice the same jump in theta in figure: 4.10.

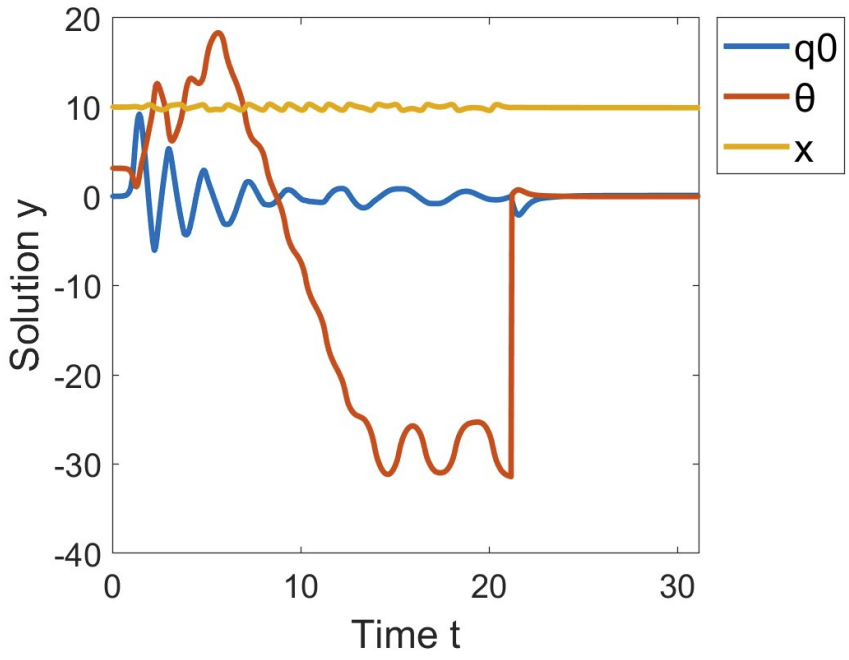

Figure: 4.7 Swing-up control and stabilization

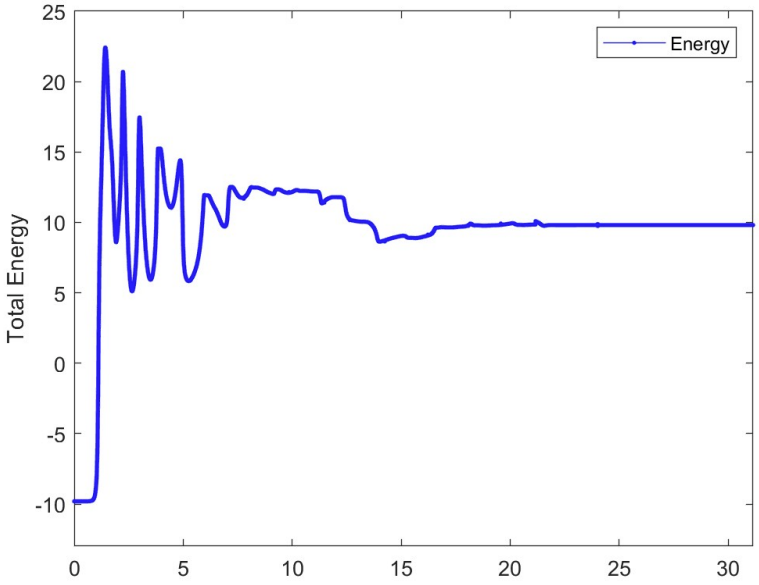

Figure: 4.8 Energy of the system

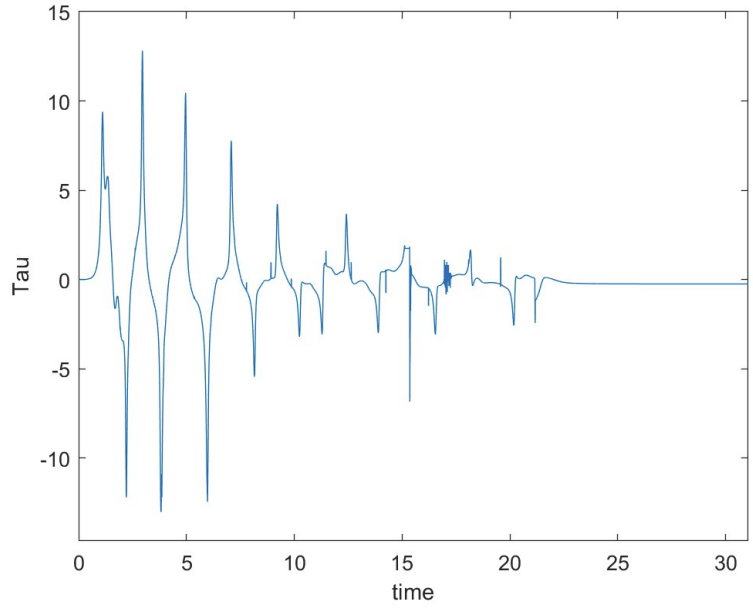

Figure: 4.9 Control input

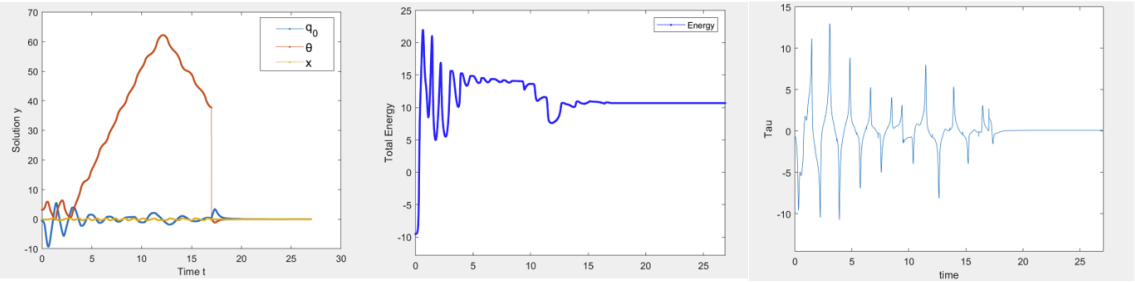

Figure: 4.10 System initialized at $x_0 = [-\frac{\pi}{6}; \pi; 0; 0.001; 0; 0]$

4.7 Summary.

In this section we derived an energy based swing-up control for the soft-robotic inverted pendulum on a cart (SIPC) system. For this we found the total energy of the system, formulated a general energy based Lyapunov function for the system, found the homoclinic orbit, derived a control input such that the Lyapunov function is non-increasing, analyzed the stability of the Lyapunov function, and used LaSalle's invariance principle to find the largest invariant set. The control input was capable of successfully bringing the system from bottom down position to the homoclinic orbit in finite time. Once the system reaches the homoclinic orbit, it will stay there (with q_o being zero, i.e., in fully elongated state, and the system will continue to oscillate along the x-axis with the pendulum continuously rotating θ continuously increasing) for all future time as expected. The experiment was repeated for several initial conditions. Even though the control input took more time to push the system into the invariant set for certain initial states, it was successfully able to do so starting at any initial condition. Even though there is a

division by $\dot{q}_0$ which could result in the control input exploding, no such thing happened during the simulation. It was also found that, the position of cart always stayed within an ε neighborhood of the starting x-position where $\varepsilon < 0.5$. Concisely written, where $x_p(0)$ is the initial x_p value, $|x_p(0) - x_p(t)| < \varepsilon$. This could be attributed to the fact that the control input is bounded, small and smooth and as a result $\dot{x}_p$ doesn't have huge jumps. It should also be noted that in the absence on a control input, because of the damping due to friction, $\dot{x}_p$ will eventually go to zero. Further, from the set of equations (89) through (93) and tuning, we get the values $k_p = 9.0,\ k_d = 2.0,\ k_e = 5.0$

Chapter-5 Feedback Linearization

5.1 Introduction

Feedback linearization is one of the earliest control strategies for controlling a nonlinear system. It has been extensively studied. It can be employed on nonlinear systems with single or multiple inputs. In addition to the control strategies employed in the previous chapters, we tried feedback linearization to control the dynamics of the system. Since the computation using the original system dynamics were expensive and time consuming, we considered the limiting case where the mass of the cart $m_p \to \infty$. As discussed in the second chapter when the mass of the cart go to infinity, the $\ddot{x}_p$ and $\dot{x}_p$ is zero and hence the system converges to the SIPR system introduced in [4]. Hence, analysis of feedback linearization was conducted on this new reduced system.

The feedback linearization approach involves transforming a nonlinear system into an equivalent linear system through a change of variables and suitable control input. Once such a transformation and control input has been identified, a regular outer loop control strategy can be deployed to achieve the required control objective. Feedback linearization for underactuated systems is an extremely tough control problem because for most of the underactuated systems, there may not exist a transformation and control input that could fully linearize the system. In such cases, we use partial feedback linearization to linearize the states that could

be linearized and analyze the zero dynamics of the non feedback linearizable states. The concept of partial feedback linearization has been extensively studied in [16], [17] and [20].

One of the earlier works in the field of feedback linearization for underactuated systems is the swing up control of an acrobot using partial feedback linearization[7]. It was already shown in [8] and [9] that acrobot is not feedback linearizable with static state feedback and nonlinear coordinate transformation. Therefore, the implementation of partial feedback linearization for swing up control and stabilization and analysis of zero dynamics were carried out. In [22] and [21] feedback linearization of quadrotor control and collocated partial feedback linearization to the position and stretching control of a planar underactuated mechanical system respectively were successfully implemented.

5.2 Simplified system and feedback linearization viability

The dynamics of the reduced system is given by

$$\ddot{q(t)} = D^{*}(q)^{-1}(\tau^{*} - (C^{*}(q,\dot{q})\dot{q} + B^{*}_{\beta}\dot{q} + K^{*}_{k}q + G^{*}(q))) \quad (95)$$

Where

$$D^{*} = \begin{bmatrix} D^{*}_{11} & D^{*}_{12} \\ D^{*}_{21} & D^{*}_{22} \end{bmatrix}, \quad C^{*} = \begin{bmatrix} C^{*}_{11} & C^{*}_{12} \\ C^{*}_{21} & C^{*}_{22} \end{bmatrix}, \quad B^{*}_{\beta} = \begin{bmatrix} \beta & 0 \\ 0 & 0 \end{bmatrix}, \quad G^{*} = \begin{bmatrix} G^{*}_{1} \\ G^{*}_{2} \end{bmatrix},$$

$$K^{*}_{k} = \begin{bmatrix} k & 0 \\ 0 & 0 \end{bmatrix}, \qquad \tau^{*} = \begin{bmatrix} \tau^{*}_{1} \\ 0 \end{bmatrix}$$

Such that,

$$D_{11}^{*} = \frac{m_p(72L^2q_0 + D^2q_0^5 + 12L^2q_0^3 - 144L^2sin(q_0) + 72L^2q_0cos(q_0))}{36q_0^5}$$

$$D_{12}^{*} = \frac{m_p(24L^2 + D^2q_0^4 + 12L^2q_0^2 - 24L^2cos(q_0) - 24L^2q_0sin(q_0))}{24q_0^4}$$

$$D_{21}^{*} = \frac{m_p(24L^2 + D^2q_0^4 + 12L^2q_0^2 - 24L^2cos(q_0) - 24L^2q_0sin(q_0))}{24q_0^4}$$

$$D_{22} = \frac{m_p(24L^2q_0 + D^2q_0^3 - 24L^2sin(q_0))}{12q_0^3}$$

$$C_{11}^{*} = \frac{-L^2m_p\dot{q_0}(12q_0 - 30sin(q_0) + 3q_0^2sin(q_0) + 18q_0cos(q_0) + q_0^3)}{3q_0^6}$$

$$C_{12}^{*} = \frac{L^2m_p\dot{\theta}(2q_0 - 3sin(q_0) + q_0cos(q_0))}{q_0^4}$$

$$C_{21}^{*} = \frac{-L^2m_p(4\dot{q_0}q_0 + \dot{q_0}q_0^2 + 2\dot{\theta}q_0^2 - 4\dot{q_0}cos(q_0) - 4q_0\dot{q_0}sin(q_0) - 3\dot{\theta}q_0sin(q_0) + q_0^2\dot{q_0}cos(q_0) + \dot{\theta}q_0^2cos(q_0))}{q_0^5}$$

$$C_{22}^{*} = \frac{-L^2m_p\dot{q_0}(2q_0 - 3sin(q_0) + q_0cos(q_0))}{q_0^4}$$

$$G_1^{*} = \frac{Lgm_p(2cos(q_0 + \theta) - 2cos(\theta) + q_0sin(q_0 + \theta) + q_0sin(\theta))}{q_0^3}$$

$$G_2^{*} = -\frac{Lgm_p(sin(\theta) - q_0cos(\theta) + q_0cos(\theta))}{q_0^2}$$

$\beta = \beta_1$ and k is the same damping from the original equation.

Now we will check whether exact linearization with state feedback is possible for the above system. From [20] suppose a system $\dot{x} = f(x) + g(x)u$ is given, then the state space exact linearization problem is solvable near a point x_0 if and only if the following conditions are satisfied.

- The matrix $\left(\left[g(x_0)\ ad_f g(x_0) \ldots . ad_f^{n-2} g(x_0)\ ad_f^{n-1} g(x_0)\right]\right)$ has rank n
- The distribution $D = span\left\{g(x_0),\ ad_f g, \ldots ad_f^{n-2} g\right\}$ is involutive near x_0

Such that for the smooth vector fields $f(x)$ and $g(x)$,

$$ad_f^k g(x) = [f, ad_f^{k-1} g](x), for\ k \geq 1\ and\ setting\ ad_f^0 g(x) = g(x)$$

where, $[f, g](x)$ is the Lie Bracket of f & g defined as $[f, g](x) = \frac{\partial g}{\partial x} f(x) - \frac{\partial f}{\partial x} g(x)$, $\frac{\partial g}{\partial x}$ and $\frac{\partial f}{\partial x}$ denotes the Jacobian matrices of mappings g and f respectively.

For the reduced SIPC system, the number of dimensions $n = 4$. First, we check the condition one. From the above analysis $g^T(x) = \left[0\ 0\ D^*(q)^{-1}\ \tau^*\right]_{4\times 1}$.

Therefore the size of the adjoint matrix(adj) $adj = \left[g(x_0)\ ad_f g(x_0) \ldots . ad_f^{n-2} g(x_0)\ ad_f^{n-1} g(x_0)\right]$ is 4×4. On substituting the condition $x_0 = [0,\ 0,\ 0,\ 0]$ we find that $rank(adj) < 4$. Since the first condition itself fails, the system is not exact feedback linearizable. We

tried the same analysis for the original SIPC system, but since the computational time complexity of the adjoint matrix is exponential, we couldn't find it.

Therefore, we tried partial feedback linearization.

5.3 Partial Feedback Linearization and normal form

The dynamics of the above system can be written as

$$D_{11}\ddot{q}_0 + D_{12}\ddot{\theta} + c_1 + \phi_1 = \tau_1 \tag{96}$$

$$D_{21}\ddot{q}_0 + D_{22}\ddot{\theta} + c_2 + \phi_2 = 0 \tag{97}$$

where c_1, ϕ_1, c_2, ϕ_2 are the elements of C-matrix and G-matrix. Now, from (97) we get,

$$\ddot{\theta} = -\ D_{22}{}^{-1}(D_{21}\ddot{q}_0 + c_2 + \phi_2) \tag{98}$$

Substituting this expression into (96) we get

$$D_{11}\ddot{q}_0 + D_{12}(-\ D_{22}{}^{-1}(D_{21}\ddot{q}_0 + c_2 + \phi_2)) + c_1 + \phi_1 = \tau_1 \tag{99}$$

$$(D_{11} - D_{12}D_{22}{}^{-1}D_{21})\ \ddot{q}_0 + c_1 - D_{12}D_{22}{}^{-1}c_2 + \phi_1 - D_{12}D_{22}{}^{-1}\phi_2 = \tau_1 \tag{100}$$

Note that the matrix $D_{11} - D_{12}D_{22}{}^{-1}D_{21}$ is the Schur's complement of D_{22} in D(q) and it is symmetric and positive definite. The control law

$$\tau_1 = (D_{11} - D_{12}D_{22}{}^{-1}D_{21})\alpha_1 + (c_1 - D_{12}D_{22}{}^{-1}c_2) + (\phi_1 - D_{12}D_{22}{}^{-1}\phi_2) \tag{101}$$

where α_1 is an additional outer-loop control term results in the normal form, $\ddot{q}_0 = \alpha_1$. Therefore the final system in normal form is given by

$$\ddot{q}_0 = \alpha_1 \tag{102}$$

$$D_{22}\ddot{\theta} + c_2 + \phi_2 = -D_{21}\alpha_1 \tag{103}$$

This system is partially feedback linearized. As we can see (102) is now linear. Therefore an outer loop control can be designed to track a trajectory for the curvature. The response for the angle (θ) is given by (103). The equation (103) represents internal dynamics with respect to an output $y = q_0$. The goal of the outer loop control then is to track a given trajectory for the curvature and at the same time excite the internal dynamics to swing the pendulum to a balancing position. In the next section we will analyze the zero dynamics of the system.

5.4 Zero Dynamics

From [16], let the output be defined as $y = h(q_1, q_2)$, then the set ϑ defined as $\vartheta = \left\{(q, \dot{q}) : h(q) = 0, \dot{h}(q) = \frac{\partial h}{\partial q}(q)\,\dot{q} = 0\right\}$ is called the zero-dynamics manifold. An outer-loop control α_1 that asymptotically stabilizes the equilibrium y = 0 makes ϑ an invariant manifold for the system. The reduced order dynamics on ϑ are called the zero dynamics.

From the previous section, the complete system in normal form with output is given by,

$$\ddot{q}_0 = \alpha_1$$

$$D_{22}\ddot{\theta} + c_2 + \phi_2 = - D_{21}\alpha_1$$

$$y = q_0 \tag{104}$$

To find the zero dynamics, we set $q_0 = 0,\ \dot{q}_0 = 0\ and\ \alpha_1 = 0$ in the above system. Therefore, the resultant system is given by,

$$D_{22-lim}\ddot{\theta} + c_{2-lim} + \phi_{2-lim} = 0 \tag{105}$$

Where,

$$D_{22-lim} = \frac{m_p(D^2+4L^2)}{12},\ c_{2-lim} = 0,\ \phi_{2-lim} = \frac{-L*g*m*sin(\theta)}{2}$$

Which gives,

$$\frac{m_p(D^2+4L^2)}{12}\ddot{\theta} - \frac{L*g*m_p*sin(\theta)}{2} = 0 \tag{106}$$

As expected, this is the dynamics of a rigid body pendulum. Since all the trajectories of this zero-dynamics manifold are periodic orbits, the equilibrium solutions are not asymptotically stable. The reduced order dynamics (106) represents the system with 2 state variables, but when one of them is fixed. Figure: 5.1 shows the phase portrait of the system defined by (106). As expected, the reduced order model has stable equilibrium points at $(2n + 1)\pi$, and unstable equilibrium points at $2n\pi$, $n \in Z$.

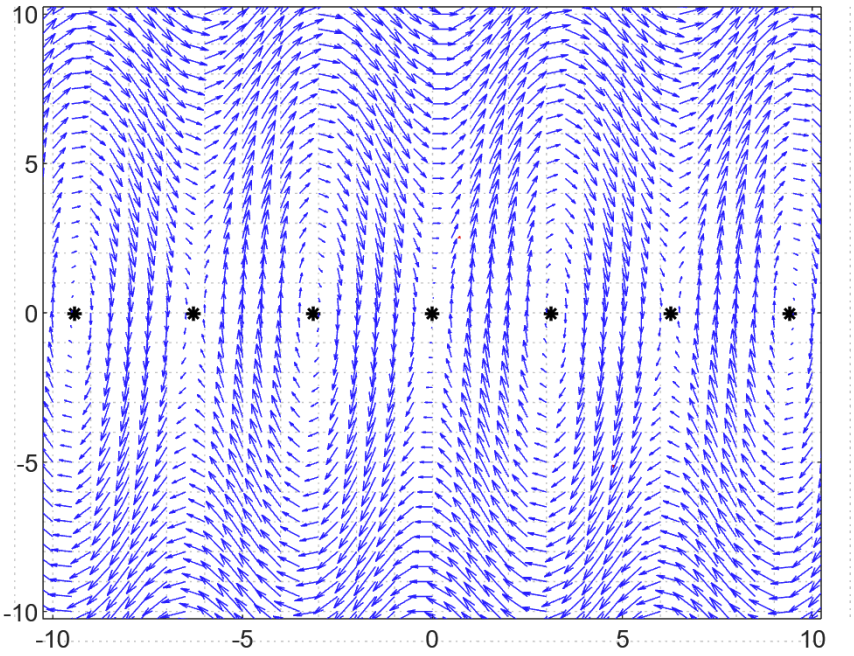

Figure: 5.1 Phase plot of zero dynamics

5.5 Summary

In this chapter, we considered a reduced version of the system and tried to feedback-linearize it. Since it was found that the system is not complete state feedback linearizable, we tried partial feedback linearization. We successfully linearized three states out of four and analyzed the zero dynamics of the system. It was found that the zero dynamics of the system is that of the rigid body pendulum

Chapter 6 Conclusion

6.1 Summary and Conclusion

To conclude, to start with, in this work we provided a thorough discussion of existing soft-robotic models and their control strategies. Then, we modeled a new oft inverted pendulum on a cart system, derived the system dynamics and the state space form. We conducted analysis on dynamics of the system for parameters. Then we linearized the system around its upright equilibrium point and studied the point's stability. Further, we discussed the controllability and stabilizability of the system. This study revealed that for the system to be stabilizable, there should exist damping between the cart and the x-axis. Next we used the Linear Quadratic Regulator to stabilize the system around the equilibrium point. Furthermore, we analytically found the region of attraction of the LQR. After this, we derived the total energy of the system, formulated an energy based Lyapunov function and derived the control law which will drive the system from any initial point to the upright equilibrium point. We also studied the stability of the control law and used LaSalle's invariance principle to ensure the convergence of trajectory to the invariant set. We also found the invariant set and proved the stability of the control law. Then we implemented a switching based control law which is the composition of swing-up and LQR. In addition to this, we studied the variability of feedback linearization, designed a partial feedback controller and found the normal form of the reduced system. We also talked about the zero-dynamics of the system.

6.2 Future Work

System modeling, control design and computer aided validation are the first few stages of any robot-control design. The next step would be to implement the system in a physical environment and study the real life practicality of the control law. In this work we have considered the soft robotic pendulum with constant curvature. Therefore, in the future work, we can extend the study towards system soft robotic arms with non-constant curvatures.

A. Appendix

A.1 Elements of Inertia Matrix

The inertia matrix D is given by,

$$D = \begin{bmatrix} D_{11} & D_{12} & D_{13} \\ D_{21} & D_{22} & D_{23} \\ D_{31} & D_{32} & D_{33} \end{bmatrix}$$

$$D_{11} = \frac{m_p(72L^2q_0 + D^2q_0^5 + 12L^2q_0^3 - 144L^2sin(q_0) + 72L^2q_0cos(q_0))}{36q_0^5}$$

$$D_{13} = \frac{Lm_p(2sin(\theta) - 2sin(q_0+\theta) + q_0cos(q_0+\theta) + q_0sin(\theta))}{q_0^3}$$

$$D_{21} = \frac{m_p(24L^2 + D^2q_0^4 + 12L^2q_0^2 - 24L^2cos(q_0) - 24L^2q_0cos(q_0))}{24q_0^4}$$

$$D_{22} = \frac{m_p(24L^2q_0 + D^2q_0^3 - 24L^2sin(q_0))}{12q_0^3}$$

$$D_{23} = \frac{Lm_p(cos(q_0+\theta) - cos(\theta) + q_0sin(\theta))}{q_0^2}$$

$$D_{31} = \frac{Lm_p(2sin(\theta) - 2sin(q_0+\theta) + q_0cos(q_0+\theta) + q_0sin(\theta))}{q_0^3}$$

$$D_{32} = \frac{Lm_p(cos(q_0+\theta) - cos(\theta) + q_0sin(\theta))}{q_0^2}$$

$$D_{33} = m_p + m_c$$

A.2 Elements of $C(q, \dot{q})$

The elements of $C(q, \dot{q})$ is given by,

$$C(q,\ \dot{q}) = \begin{bmatrix} C_{11} & C_{12} & C_{13} \\ C_{21} & C_{22} & C_{23} \\ C_{31} & C_{32} & C_{33} \end{bmatrix}$$

$$C_{11} = \frac{-L^2 m_p \dot{q_0}(12q_0 - 30sin(q_0) + 3q_0^2 sin(q_0) + 18q_0 cos(q_0) + q_0^3)}{3q_0^6}$$

$$C_{12} = \frac{L^2 m_p \dot{\theta}(2q_0 - 3sin(q_0) + q_0 cos(q_0))}{q_0^4}$$

$$C_{13} = 0$$

$$C_{21} = \frac{-L^2 m_p(4\dot{q_0} + \dot{q_0} q_0^2 + 2\dot{\theta} q_0^2 - 4\dot{q_0} cos(q_0) - 4\dot{q_0} q_0 sin(q_0) - 3\dot{\theta} q_0 sin(q_0) + q_0^2 \dot{q_0} cos(q_0) + \dot{\theta} q_0^2 cos(q_0))}{q_0^5}$$

$$C_{22} = \frac{-L^2 m_p \dot{q_0}(2q_0 - 3sin(q_0) + q_0 cos(q_0))}{q_0^4}$$

$$C_{23} = 0$$

$$C_{31} = \frac{-Lm_p(6\dot{q_0} sin(\theta) - 6\dot{q_0} sin(q_0 + \theta) + q_0^2 \dot{q_0} sin(q_0 + \theta) + \dot{\theta} q_0^2 sin(q_0 + \theta) + \dot{\theta} q_0^2 sin(\theta) + 4L\dot{q_0} cos(q_0 + \theta) + 2\dot{\theta} q_0 cos(q_0 + \theta)}{q_0^4}$$

$$+ \frac{2Lm_p \dot{\theta} q_0 cos(\theta) - 2\dot{q_0} q_0 cos(\theta)}{q_0^4}$$

$$C_{32} = \frac{-Lm_p(2\dot{q_0} cos(q_0 + \theta) - 2\dot{q_0} cos(\theta) - \dot{\theta} q_0^2 cos(\theta) + \dot{q_0} q_0 sin(q_0 + \theta) + q_0 \dot{\theta} sin(q_0 + \theta) + \dot{q_0} q_0 sin(\theta) - \dot{\theta} q_0 sin(\theta))}{q_0^3}$$

$$C_{33} = 0$$

A.3 Lyapunov Stability

Given the nonlinear system defined by equation $\dot{x}(t) = f(x(t))$, suppose that $x = 0 \in \Re^n$ is an equilibrium. Then the null solution $x(t_0) = 0$ is said to be

- stable if and only if, for any $\varepsilon > 0$ there exist $\delta = \delta(\varepsilon) > 0$ such that $||x(t_0)|| < \delta \, implies \, ||x(t)|| < \varepsilon$ for all $t > t_0$
- asymptotically stable if x = 0 is stable and, in addition, $||x(t_0)|| < \delta \, implies \, ||x(t)|| \to 0 \, as \, t \to \infty$
- unstable if it is not stable.

The stability, respectively, asymptotic stability, is said to be global if the corresponding conditions hold for every initial condition $x(t_0) \in \Re^n$

A.4 Schur's Complement

Let M be a $(p + q) \times (p + q)$ matrix partitioned into sub-blocks as

$$M = \begin{bmatrix} A & B \\ C & D \end{bmatrix}$$

in which A, B, C, and D are, respectively $p \times p$, $p \times q$, $q \times p$, $and \, q \times q$ sub-matrices. Assuming that D is invertible, the Schur complement of the block D in the matrix M is the $p \times p$ matrix

$$D = A - BD^{-1}C$$

Further,

- If M is a symmetric, positive definite matrix, then so is the Schur complement of D in M
- The determinant of M is $det(D) * det(A - BD^{-1}C)$
- The rank of M is equal to $rank(D) + rank(A - BD^{-1}C)$

References

[1]. Kim S, Laschi C, Trimmer B. Soft robotics: a bioinspired evolution in robotics. Trends Biotechnol. 2013 May;31(5):287-94. doi: 10.1016/j.tibtech.2013.03.002. Epub 2013 Apr 12. PMID: 23582470.

[2] D. Rus and M. T. Tolley, “Design, fabrication and control of soft robots,” Nature, vol. 521, no. 7553, pp. 467–475, 2015.

[3] C. Della Santina, R. K. Katzschmann, A. Bicchi, and D. Rus, “Model based dynamic feedback control of a planar soft robot: trajectory tracking and interaction with the environment,” The International Journal of Robotics Research, vol. 39, no. 4, pp. 490–513, 2020.

[4]. L. Weerakoon and N. Chopra, "Swing up Control of a Soft Inverted Pendulum with Revolute Base," *2021 60th IEEE Conference on Decision and Control (CDC)*, Austin, TX, USA, 2021, pp. 685-690, doi: 10.1109/CDC45484.2021.9683691.

[5] C. Della Santina, “The soft inverted pendulum with affine curvature,” in 2020 59th IEEE Conference on Decision and Control (CDC). IEEE, 2020, pp. 4135–4142.

[6] C. Della Santina and D. Rus, “Control oriented modeling of soft robots: the polynomial curvature case,” IEEE Robotics and Automation Letters, vol. 5, no. 2, pp. 290–298, 2019.

[7] Mark W. Spong, Swing up control of the acrobot using partial feedback linearization*, IFAC Proceedings Volumes, Volume 27, Issue 14, 1994, Pages 833-838, ISSN 1474-6670, https://doi.org/10.1016/S1474-6670(17)47404-0.

[8] Bortoff. S (1992). Pseudo linearization using Spline Functions with Application to the acrobot. Ph.D. Thesis , Dept. of Electrical and Computer Engineering. University of Illinois at Urbana- Champaign.

[9] Bortoff, S.A. and M.W. Spong (1992). Observer based pseudo-linearization using splines: The rolling acrobot example. ASME Winter Annual Meeting. Anaheim, CA.

[10] M. W. Spong, “The swing up control problem for the acrobot,” IEEE control systems magazine, vol. 15, no. 1, pp. 49–55, 1995.

[11] M. W. Spong, “Swing up control of the acrobot,” in Proceedings of the 1994 IEEE International Conference on Robotics and Automation, 1994, pp. 2356–2361 vol.3.

[12] M. W. Spong and L. Praly, “Control of underactuated mechanical systems using switching and saturation,” in Control Using Logic-Based Switching, A. Stephen Morse, Ed. Berlin, Heidelberg: Springer Berlin Heidelberg, 1997, pp. 162–172.

[13] I. Fantoni, R. Lozano and M. W. Spong, "Energy based control of the Pendubot," in *IEEE Transactions on Automatic Control*, vol. 45, no. 4, pp. 725-729, April 2000, doi: 10.1109/9.847110.

[14] Rogelio Lozano, Isabelle Fantoni, Dan J. Block, Stabilization of the inverted pendulum around its homoclinic orbit, Systems & Control Letters, Volume 40, Issue 3, 2000, Pages 197-204, ISSN 0167-6911, https://doi.org/10.1016/S0167-6911(00)00025-6.
(https://www.sciencedirect.com/science/article/pii/S0167691100000256)

[15] I. Fantoni, R. Lozano, F. Mazenc, and A. Annaswamy, "Stabilization of a two-link robot using an energy approach," in 1999 European Control Conference (ECC). Karlsruhe, Germany, 1999, pp. 2886–2891.

[16] M. W. Spong, S. Hutchinson, and M. Vidyasagar, Robot modeling and control. John Wiley & Sons, Inc., 2006.

[17] H.K. Khalil, Non-Linear Systems, 2nd ed., Prentice-Hall, Englewood Cliffs, NJ, 1996.

[18] João P. Hespanha, *Linear Systems Theory, 2nd edition*, Princeton University Press, 2018

[19] Najafi, E., Babuška, R. & Lopes, G.A.D. A fast sampling method for estimating the domain of attraction. *Nonlinear Dyn* **86**, 823–834 (2016). https://doi.org/10.1007/s11071-016-2926-7

[20] Alberto. Isidori. Nonlinear Control Systems. Springer-Verlag, Berlin, third edition, 1995.

[21] Fenili A. Mathematical modeling and partial feedback linearization control of a constrained and underactuated space tether. *Journal of Vibration and Control*. 2022;0(0). doi:10.1177/10775463221084402

[22] S. A. Al-Hiddabi, "Quadrotor control using feedback linearization with dynamic extension," *2009 6th International Symposium on Mechatronics and its Applications*, Sharjah, United Arab Emirates, 2009, pp. 1-3, doi: 10.1109/ISMA.2009.5164788.

[23] Xin Xin, Analysis of the Energy Based Swing-up Control for a Double Pendulum on a Cart, IFAC Proceedings Volumes, Volume 41, Issue 2, 2008, Pages 4828-4833, ISSN 1474-6670, ISBN 9783902661005, https://doi.org/10.3182/20080706-5-KR-1001.00811.

[24] Spong, Mark W.. "Partial feedback linearization of underactuated mechanical systems." *Proceedings of IEEE/RSJ International Conference on Intelligent Robots and Systems (IROS'94)* 1 (1994): 314-321 vol.1.

[25] Mark W. Spong, Energy Based Control of a Class of Underactuated Mechanical Systems, IFAC Proceedings Volumes, Volume 29, Issue 1, 1996, Pages 2828-2832, ISSN 1474-6670, https://doi.org/10.1016/S1474-6670(17)58105-7.

[26] Rogelio Lozano, Isabelle Fantoni, Passivity Based Control of the Inverted Pendulum, IFAC Proceedings Volumes, Volume 31, Issue 17, 1998, Pages 143-148, ISSN 1474-6670, https://doi.org/10.1016/S1474-6670(17)40325-9.

[27] S. Nakatani and H. Date, "Swing up Control of Inverted Pendulum on a Cart with Collision by Monte Carlo Model Predictive Control," *2019 58th Annual Conference of the Society of Instrument and Control Engineers of Japan (SICE)*, Hiroshima, Japan, 2019, pp. 1050-1055, doi: 10.23919/SICE.2019.8859912.

[28] M. W. Spong and D. J. Block, “The pendubot: a mechatronic system for control research and education,” in Proceedings of 1995 34th IEEE Conference on Decision and Control, vol. 1, 1995, pp. 555–556 vol.1.